



VICTORIA UNIVERSITY
MELBOURNE AUSTRALIA

*Prediction of the amount of sediment Deposition in
Tarbela Reservoir using machine learning
approaches*

This is the Published version of the following publication

Hassan, Shahzal, Shaukat, Nadeem, Ahmad, Ammar, Abid, Muhammad, Hashmi, Abrar, Shahid, Muhammad Laiq Ur Rahman, Rajabi, Zohreh and Tariq, Muhammad Atiq Ur Rehman (2022) Prediction of the amount of sediment Deposition in Tarbela Reservoir using machine learning approaches. *Water (Switzerland)*, 14 (19). ISSN 2073-4441

The publisher's official version can be found at
<https://www.mdpi.com/2073-4441/14/19/3098>
Note that access to this version may require subscription.

Downloaded from VU Research Repository <https://vuir.vu.edu.au/46244/>

Article

Prediction of the Amount of Sediment Deposition in Tarbela Reservoir Using Machine Learning Approaches

Shahzal Hassan ¹, Nadeem Shaukat ^{2,3} , Ammar Ahmad ², Muhammad Abid ^{4,5}, Abrar Hashmi ⁶ , Muhammad Laiq Ur Rahman Shahid ⁷ , Zohreh Rajabi ⁸  and Muhammad Atiq Ur Rehman Tariq ^{8,9,*} 

- ¹ Department of Mechanical Engineering, Pakistan Institute of Engineering & Applied Sciences, Nilore, Islamabad 45650, Pakistan
- ² Center for Mathematical Sciences (CMS), Pakistan Institute of Engineering & Applied Sciences, Nilore, Islamabad 45650, Pakistan
- ³ Department of Physics and Applied Mathematics (DPAM), Pakistan Institute of Engineering & Applied Sciences, Nilore, Islamabad 45650, Pakistan
- ⁴ Department of Mechanical Engineering, COMSATS University Islamabad, Wah Campus, Wah Cantt 47040, Pakistan
- ⁵ Interdisciplinary Research Center, COMSATS University Islamabad, Wah Campus, Wah Cantt 47040, Pakistan
- ⁶ Department of Electrical Engineering, Capital University and Technology, Islamabad 45750, Pakistan
- ⁷ Department of Electronic Engineering, University of Engineering and Technology Taxila, Rawalpindi 46000, Pakistan
- ⁸ Institute for Sustainable Industries & Liveable Cities, Victoria University, P.O. Box 14428, Melbourne 8001, Australia
- ⁹ College of Engineering, IT & Environment, Charles Darwin University, Darwin 0810, Australia
- * Correspondence: atiq.tariq@yahoo.com



Citation: Hassan, S.; Shaukat, N.; Ahmad, A.; Abid, M.; Hashmi, A.; Shahid, M.L.U.R.; Rajabi, Z.; Tariq, M.A.U.R. Prediction of the Amount of Sediment Deposition in Tarbela Reservoir Using Machine Learning Approaches. *Water* **2022**, *14*, 3098. <https://doi.org/10.3390/w14193098>

Academic Editors: Sanjay Giri and Biswa Bhattacharya

Received: 16 August 2022

Accepted: 26 September 2022

Published: 1 October 2022

Publisher's Note: MDPI stays neutral with regard to jurisdictional claims in published maps and institutional affiliations.



Copyright: © 2022 by the authors. Licensee MDPI, Basel, Switzerland. This article is an open access article distributed under the terms and conditions of the Creative Commons Attribution (CC BY) license (<https://creativecommons.org/licenses/by/4.0/>).

Abstract: Tarbela is the largest earth-filled dam in Pakistan, used for both irrigation and power production. Tarbela has already lost around 41.2% of its water storage capacity through 2019, and WAPDA predicts that it will continue to lose storage capacity. If this issue is ignored for an extended period of time, which is not far away, a huge disaster will occur. Sedimentation is one of the significant elements that impact the Tarbela reservoir's storage capacity. Therefore, it is crucial to accurately predict the sedimentation inside the Tarbela reservoir. In this paper, an Artificial Neural Network (ANN) architecture and multivariate regression technique are proposed to validate and predict the amount of sediment deposition inside the Tarbela reservoir. Four input parameters on yearly basis including rainfall (R_a), water inflow (I_w), minimum water reservoir level (L_r), and storage capacity of the reservoir (C_r) are used to evaluate the proposed machine learning models. Multivariate regression analysis is performed to undertake a parametric study for various combinations of influencing parameters. It was concluded that the proposed neural network model estimated the amount of sediment deposited inside the Tarbela reservoir more accurately as compared to the multivariate regression model because the maximum error in the case of the proposed neural network model was observed to be 4.01% whereas in the case of the multivariate regression model was observed to be 60.7%. Then, the validated neural network model was used for the prediction of the amount of sediment deposition inside the Tarbela reservoir for the next 20 years based on the time series univariate forecasting model ETS forecasted values of R_a , I_w , L_r , and C_r . It was also observed that the storage capacity of the Tarbela reservoir is the most influencing parameter in predicting the amount of sediment.

Keywords: Tarbela reservoir; sedimentation; artificial neural network; forecasting; multivariate regression

1. Introduction

Reservoir sedimentation is a primary concern in all reservoirs across the world. It is one of the major drawbacks associated with storage reservoirs. The capacity of reservoirs worldwide is decreased by 0.5–1% annually due to reservoir sedimentation [1]. The

life of a reservoir is usually calculated at the point when it loses its storage capacity by approximately 80 percent to the sediments [2]. Apart from impacting the reservoir's life, sedimentation also has environmental effects on the lands downstream of the reservoir. Moreover, increasing sediment concentration impacts the life of structures downstream of the reservoir like tunnels, turbines for hydropower generation, etc. Pakistan uses the 250 km² catchment area of Tarbela Dam, one of the largest earth-filled dams in the world, for irrigation and power generation. It is situated on the Indus River and is 96.6 km long [2,3]. Its initial storage capacity has dropped by 41.2%, according to the annual sedimentation report of the Water and Power Development Authority (WAPDA) of Pakistan [4]. Since it was first commissioned, several sedimentation estimation studies have been performed by consultants using sediment rating curves (SRC) [5].

Reservoirs are usually filled by the water coming in rivers from snowmelt and rainfall through the watershed. Rivers come through hilly areas and thus carry a huge amount of sediment in the form of sand, silt, and clay usually with them. Some of these sediments can be absorbed by the vegetation, in those hilly areas. The sediment that is not absorbed, travels along the river over long distances. Water needs a particular velocity to carry the sediments along with it. When water enters the reservoir, its speed decreases. Hence, its sediment carrying capacity reduces. Thus, it deposits a large amount of sediment there, but its deposition is not uniform. Heavier particles deposit in the upper reaches of the reservoir (away from the reservoir) while the lighter particles deposit in the lower reaches of the reservoir (near the reservoir), thus forming a sloped shape known as "Delta". The reservoir water level changes in the whole year from high head conditions when the reservoir is filled to low head conditions when the reservoir level is decreasing. Every year when the reservoir level reduces, water above this delta erodes the sediment there and carries some quantity. It also deposits some of it near the reservoir, causing the delta to advance towards the tunnel inlets while entraining some of the particles in flow and carrying the remaining particles. Due to their high velocity, these particles cause the walls of the tunnel and other mechanical structures like Turbines to erode. With the advancement of the delta, the concentration of sediment in the outflow increases, which can shorten the life of tunnels and turbines. Also, the storage capacity reduces every year due to the advancement of the delta [6].

The sediment load is estimated to be 200 million tons per year, according to Roca [7]. These calculations overestimated the Tarbela reservoir's predicted lifespan, which had been previously estimated at 30 years. Sedimentation is influenced by the reservoir's storage capacity, operational level, and annual rainfall, further complicating the relationship. Pakistan is an agricultural country and relies on water storage reservoirs for irrigation and a major part of power production (approximately 24% of total power). Tarbela is the largest earth-filled dam in Pakistan used for both power generation and irrigation purposes. Tarbela is losing its water storage capacity like any other water storage reservoir due to sedimentation. When it is difficult to construct new water storage reservoirs in Pakistan due to the financial situation, it becomes very essential to keep all the existing storage reservoirs in optimal operational condition, and for that, the accurate prediction of sedimentation is necessary [7].

2. Literature Review

Abrahat and White [8] conducted experiments to determine whether a back-propagation artificial neural network could develop a composite model of sediment transfer under various farming and land management conservation regimes. It was found that a neural network solution can overcome the constraints of conventional models. In order to forecast and estimate sediment concentration values, Cigizoglu [9,10] employed artificial neural networks. They discovered that the forecasted values were quite similar to the actual ones. Hydrodynamic and ANN models were combined by Dibike et al. [11]. Navigation depth, water level, flow velocity, flow direction, and flow rate were all predicted using the trained ANN model, which had been trained using data samples from the hydrodynamic model.

The relationship between the Three Gorges Reservoir's (TGR) effectiveness at flushing out sediment and its affecting variables, including inflow of water, inflow of sediment, sediment discharge, and water head, was examined by Li et al. [12]. Tarar et al. [13] used wavelet artificial neural networks and SRC to model sediment transport in Tarbela Reservoir to determine the boundary conditions for the sediment load in a one-dimensional Hydrologic Engineering Center River Analysis System. Rashid et al. [14] discovered that the reservoir storage depletion can be decreased after using the above-mentioned model to assess the impact of various management research works on the Tarbela reservoir's lifespan. The effect of reservoir operation on sediment deposition was also examined by Petkovsek and Roca [15], who discovered that delta movement may be halted by increasing the minimum reservoir level. The Tarbela reservoir's storage losses due to sedimentation were incorporated into a new model created by Khan and Tingsanchali [16]. Arfan et al. [17] found that the mean, maximum, and minimum flows on an annual basis at the Tarbela Dam on the Indus River fell deeply from 1986 to 2010 compared to 1961 to 1985. In the Upper Indus Basin, Ul Hussan et al. [18] looked at trends in suspended sediment concentrations and water discharge. For the purpose of predicting rainfall-runoff, Chiang et al. [19] have presented a systematic comparison of two fundamental types of neural networks, static and dynamic. For the static network, the real-time recurrent learning (RTRL) technique was utilized, and for the dynamic-feedback network, two back-propagation (BP) learning optimization strategies, the conventional BP and conjugate gradient (CG) approaches, were used. By employing the Monte Carlo simulations using data exhibiting defined mathematical correlations, it has been possible to compare the various approaches in a more acceptable way [20,21].

The recent decades in the north of the East European Plain have been characterized by Gusarov et al. [22] with notable shifts in climate and land cover in the Vyatka River basin. Török et al. [23] used the most popular empirical model's application range. However, it was frequently constrained by hydraulic and sedimentological characteristics, making it difficult to apply a numerical model to complex situations. Rodríguez-Blanco et al. [24] have used the Soil and Water Assessment Tool (SWAT) model to evaluate the short-term and long-term consequences of expected changes in temperature, rainfall, and CO₂ concentration on sediment yield in a small rural catchment located in NW Spain. The river basin has been explored along with the key findings of the hydrological analysis. For the analysis of the flood event using the suggested methodology, the photographic sampling technique and assessment of the sediment size distribution have been presented by Di Francesco et al. [25]. Xiao et al. [26] used the location-weighted landscape contrast index (LCI), which is based on the "source-sink" hypothesis, with this, it has been possible to determine how the sediment yield in the Poyang Lake drainage basin responds to changes in plant cover. The diurnal change of the suspended sediment content in the East China Sea, with an emphasis on Hangzhou Bay, has been studied by Yang et al. [27] using a coupled hydrodynamic-ecological model for regional and shelf seas (COHERENS).

In the Shiwen River in southern Taiwan, Tfwala et al. [28] investigated how artificial neural networks (ANNs) might improve the accuracy of stream flow-suspended discharge relationships during storm occurrences. Guerrero et al. [29] have taken care of the practical necessity to assess the viability of various acoustic approaches in various sections of the Parana River in Argentina and a river segment of the Danube River in Hungary. Data from the observed stream flow, sediment concentration, and rain gauge readings during rainfall events in the Goodwin Creek Experimental Watershed in Mississippi, USA, were used by Yin et al. [30]. Nabi et al. [31] explained the primary hydrological and sediment transport-related processes using SWAT watershed modeling to evaluate the efficacy of soil and water conservation buildings to prevent soil erosion. The physically-based EROSION-3D model (Jürgen Schmidt, Berlin, Germany) and sediments confined in a small reservoir was contrasted by Némethová et al. [32]. Through six years of high-resolution weekly monitoring on an Appalachian hill slope, with a focus on the seasonal impact, the impact of precipitation parameters on soil erosion has been studied by Luffman et al. [33]. In the

presence of a time-dependent sedimentation/erosion process, a second-order semi-implicit numerical technique based on the approach has been developed by Tavelli et al. [34]. The total sediment transport rate formula of Yang's arithmetic coefficients has been transformed into fuzzy numbers by Kaffas et al. [35], resulting in a fuzzy relationship that has produced a fuzzy band of in-stream sediment concentration. Xin et al. [36] observed simulated rainfall experiments to observe the infiltration processes of black soil slopes under bare and residue-covered situations. A study of the impact of ponds in limnologically rich basins on soil erosion and sediment transport has been reported by Al Sayah et al. [37]. The construction of a debris-blocking dam has been studied by Wang et al. [38] under various downstream riverbed slope conditions. Typhoons and torrential rains have caused major landslides and debris flows in the Chenyulan watershed. The TUSLE and landslide volume estimation were incorporated by Lu et al. [39] into the SWAT model as SWAT-Twn. Song et al. [40] developed a method to evaluate conduit flow. The technology could easily calculate complex features and estimate a conduit's discharge capacity. According to Aksoy et al. [41], as the number of dams in a watershed increases, a large portion of the sediment fluxes are retained in the reservoirs and do not reach the sea in the same quantity or quality, having an impact on the coastal geomorphodynamics. Hauer [42] demonstrated many possibilities for integrating better process knowledge into tactical or numerical tools for reservoir operations. The results of the study enabled a substantive discussion about if and how hydrological thresholds may be included in management practice for strategic management. In a laboratory microcosm experiment, Patil et al. [43] investigated the effectiveness of *Bacillus subtilis* zeolite (BZ) as a capping material to limit sediment contaminants. Reisenbüchler et al. [44] demonstrated that, under specific circumstances, sediment might be more successfully re-mobilized and conveyed through the HPP by testing various reservoir operation modes. According to Sotiri et al. [45], the sediment yield model is primarily responsible for the most significant causes that lead to inconsistencies in the Passana sediment budget case. Jothiprakash and Garg proposed the typical neural network architecture for the predicted value of sediments accumulated inside the Gobindsagar reservoir [46]. In the Changjiang River estuary and nearby coastal waters, Chen et al. [47] discussed temporal fluctuations of fine suspended sediment concentration. Effects of intermittent heavy rainstorm events on suspended sediments were addressed by Wang et al. [48]. Tenget et al. [49] discovered Taiwan's exposure to flood disasters over the previous 25 years. The significance of tiny mountainous rivers for geomorphic/tectonic control of sediment discharge to the ocean was examined by Milliman et al. [50]. In order to estimate suspended sediment concentrations for upcoming flux calculations, Horowitz [51] has conducted a number of evaluations of the sediment rating-curve method for the estimation of suspended sediment fluxes using data from long-term, daily sediment-measuring sites in large, medium, and small river basins in the USA and Europe. Using probability sampling, Thomas et al. [52] calculated total suspended sediment yield. In a typhoon-prone location, Wang et al. [53] used a time-lagged recurrent network to estimate episodic event suspended sediment burden. For modeling the rainfall runoff caused by a typhoon, Chen et al. [54] adopted an artificial neural network approach. For the prediction of missing flow records, Tfwala et al. [55] used a multilayer perceptron and a coactive neuro-fuzzy inference system. Melesse et al. [56] found suspended sediment load prediction of river systems using an artificial neural network approach. For modeling evapotranspiration, Kisi et al. [57] built generalized regression neural networks. Based on climate information, Wang et al. [58] computed and modeled agricultural yields in Burkina Faso. Support vector machines were utilized by Lin et al. [59] to forecast long-term discharge. An artificial neural network's structure optimization and input selection were carried out by Leahy et al. [60] to predict river level.

Recurrent neural networks with hessian-free optimization were created by Martens and Sutskever [61] for the estimation of sediment deposition. Using neural differential evolution (NDE), multi-layer perceptron (MLP), and radial basis function (RBF) models, Feyzolahpour et al. [62] evaluated the concentration of suspended sedimentation. To

perform training and prediction on the monthly suspended sediment concentration data from Huayuankou hydrological station from 1960 to 2014, Zhang and Yang [63] constructed a coupling model based on CEEMDAN-GRU. The findings showed that the Huayuankou hydrographic station's monthly suspended sediment content was declining year over year, and the period and trend were compatible with the measured data. Froehlich and Giri [64] have developed a neural network model to calculate the expected amount of capacity loss using data on storage loss caused by siltation in 220 reservoirs in India. The predictions are based on the catchment area, reservoir surface area, initial storage volume, time since the escheatment was first filled, and a stream flow indicator. The model offers a close fit to the data and allows for an easy calculation of reservoir half-life, which provides a measure of when sedimentation has a significant impact on a reservoir's functioning. The multiple linear regression (MLRg), Multilayer perceptrons (Levenberg-Marquardt (LM), Scaled Conjugate Descent (SCG), and Broyden-Fletcher-Goldfarb-Shanno Quasi-Newton (BFGS)), and Radial Basis Function (RBF) have been used by Uca et al. [65] to predict daily suspended sediment discharge in the Jenderam catchments of Selangor, Malaysia. Based on the accuracy with which MLRg, LM, SCG, BFGS, and RBF model the non-linear complex behavior of suspended sediment responses to rainfall, water depth, and discharge in small catchment areas, a suitable ANN model architecture was developed by Nourani [66], and the performance of ANN's application to problems involving the estimation of sediment load from runoff was compared to two conventional methods. When compared to the other methods, an ANN model with three neurons in the input layer, representing the quantity of discharge on the current day, one day, and two days before the date of observed suspended sediment load data, and six neurons in the hidden layer, produced the most promising results. It was suggested that using a wide range of well-established data may increase the accuracy of the ANN results. Sokchhay and Tadashi [67] simulated the monthly average suspended sediment load (SSLm) of four catchments using an artificial neural network (ANN), and assessed the application of the calibrated ANN (Cal-ANN) models in three ungauged catchment representatives before using them to predict SSLm of three actual ungauged catchments (AUC) in the Tonle Sap River Basin; they also estimated annual SSL (SSLA) of each AUC with and without dam-reservoirs. Qian et al. [68], hybrid ML models have a long training time, especially when dealing with complex problems. In comparison to standalone ML models, hybrid ML models require far more input parameters to be considered during training. This frequently limits the development and application of hybrid machine learning models. Furthermore, complex architecture and an unknown optimal number of clusters have been identified by Fallah et al. [69] as drawbacks of using hybrid ML models. The convolutional neural network is a type of ML algorithm that has received little attention in the context of SSL prediction (CNN). The CNN has shown a lot of promise in other fields. In Carlisle, United Kingdom, Kabir et al. [70] created a CNN to predict flood depths. This study's CNN model was trained using outputs from a two-dimensional (2D) hydraulic model. The performance of the CNN model was compared to that of a support vector regression (SVR) model. Haurum et al. [71], investigated the use of CNN in estimating water levels in sewer pipes in Denmark. Models based on the decision tree algorithm were also trained and tested for performance comparison with the CNN model. In this study, the estimation problem is treated as a classification and regression problem. In the context of estimating water levels, this study demonstrates that CNN models outperform decision tree models. Ni and Ma [72] investigated the feasibility of using a CNN-based model to predict power generation from a marine wave energy converter (WEC) system using a double buoy oscillating device (OBD). The CNN was trained and tested using a multi-input approach. According to the study, the proposed CNN model outperforms the ANN and regression models in the prediction of marine wave power generation.

Samantaray and Sahoo [73] assessed the sediment load at two gauging stations in the Indian River basin of the Mahanadi. Here, a novel Support Vector Machine with Whale optimization algorithm has been used to forecast suspended sediment concentration for

the proposed study area and has been compared with a traditional Radial Basis Function Network (RBFN), Support Vector Machine, and Support Vector Machine-Particle Swarm Optimization (SVM-PSO) model. For the prediction of suspended sediments in the Johor River in Malaysia, Nouar et al. [74] developed an LSTM model. Daily sediment and discharge data were used to train the prediction model. The model was trained and verified on 80% of the data, and on the remaining 20%, it was tested. The prediction of suspended sediment was examined using four alternative models, including ElasticNet Linear Regression, MLP neural network, Extreme Gradient Boosting, and Long Short-Term Memory. The standalone machine learning approaches can accurately predict the amount of sediment in the reservoirs compared to conventional multiple regression approaches. However, despite being able to forecast the amount of sediment, standalone machine learning approaches have a number of drawbacks that should be highlighted. In general, it is clear that hybrid ML models have been developed to be more accurate and reliable than independent ML models. However, in the present study, standalone machine learning approaches have been implemented to predict the amount of sediment.

According to WAPDA, Tarbela has already lost approximately 41.2% of its water storage capacity by 2019 and is continuously losing its storage capacity [3]. If this situation is ignored for a long time, it will cause a serious crisis and that time is not very far. Sedimentation is one of the important factors impacting the storage capacity of the Tarbela reservoir. Therefore, it is a dire need to accurately predict the sedimentation inside the Tarbela reservoir, which has not been done prior to this work. Till now, sedimentation inside the Tarbela was estimated using linear techniques known as sediment rating curves, which are the linear relationship between sedimentation and water discharge. However, with time, it has been proven that these predictions were not accurate. Therefore, a need to find better techniques to predict sedimentation inside the Tarbela reservoir is evident. Artificial Neural Networks (ANN) have proven very useful for modeling complex phenomena without modeling the underlying physics. So, ANN will be useful for accurately predicting the sediments deposited inside the Tarbela reservoir.

Based on the previous studies, it is found that the accurate predictions of sedimentation inside the Tarbela reservoir using ANN have not been done prior to this work. The ultimate objectives of this study are:

1. To find the amount of sediment deposited inside the Tarbela reservoir using the proposed artificial neural network model and the multivariate regression model considering four yearly influencing factors: R_a , I_w , L_r , and C_r .
2. To make future predictions of the sedimentation volume inside the Tarbela reservoir using trained ANN based on the time series univariate forecasting model ETS forecasted values of R_a , I_w , L_r , and C_r .

The results for the Tarbela reservoir were compared with the multivariate regression model's results, which were obtained using the same inputs, and the actual amount of sediment deposited quoted by WAPDA. In comparison to the regression model, it was found that the proposed neural network model can predict the sediments deposited inside the Tarbela reservoir more accurately. The collection of data for sedimentation retained inside both the reservoirs considered in this study, the model developed, model validation, and the prediction of the amount of sediment are discussed in detail in the subsequent sections.

3. Materials and Methods

The Tarbela reservoir's annual deposit of sediments was validated using the proposed ANN model. To estimate the amount of sediment deposited, a multivariate regression model was first used in conjunction with various combinations of the yearly basis values input parameters including rainfall, water inflow, reservoir storage capacity, and the minimum water level inside the reservoir. The results obtained by multivariate regression and neural network model were compared with the actual amount of sediment quoted by WAPDA. The effect of various combinations of influencing parameters in the prediction

of the sediments deposited was studied. The flow of the validation and prediction of the amount of sediment inside the Tarbela reservoir is given in Figure 1 below.

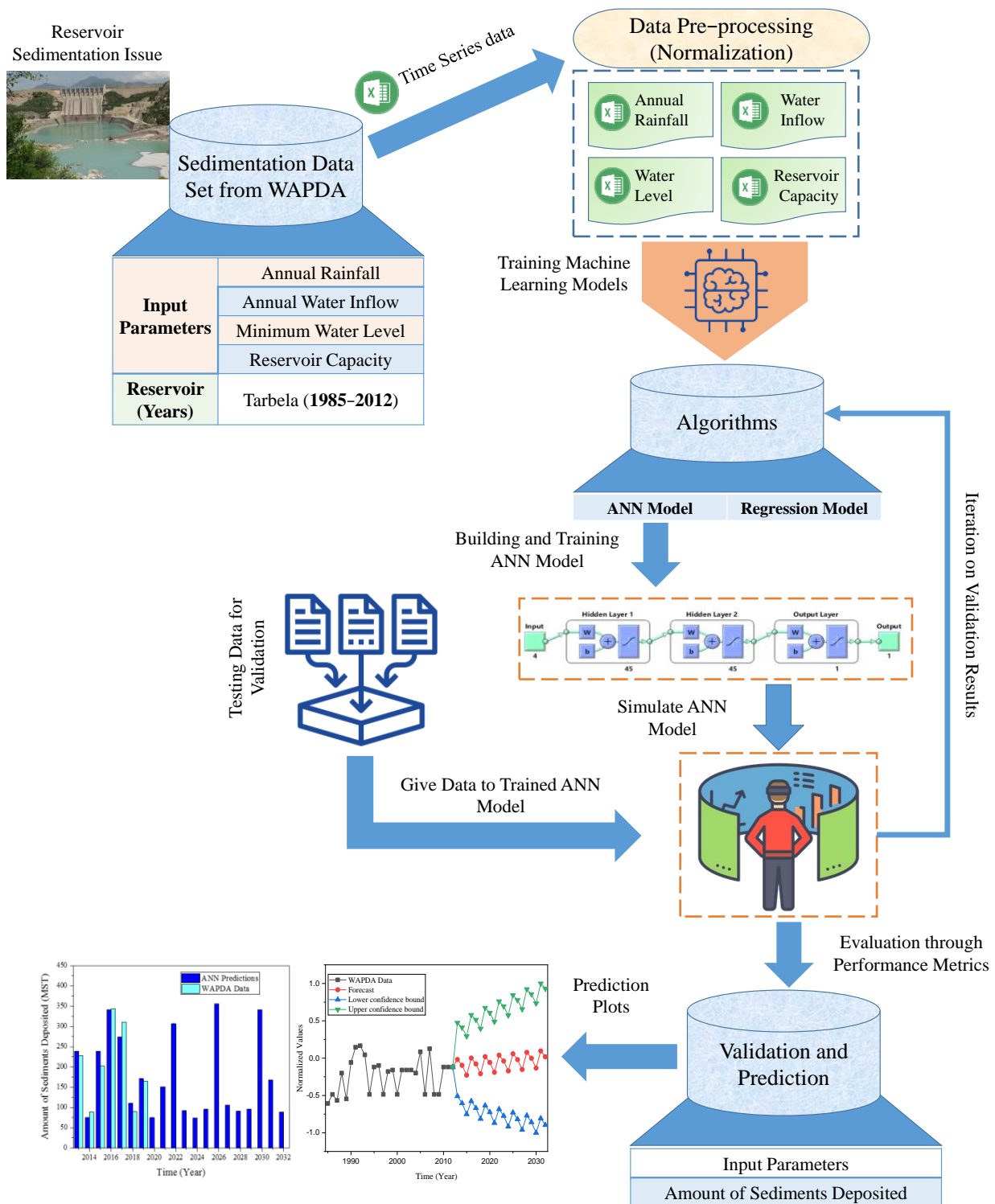


Figure 1. Schematic flow procedure for the pre-processing of data and implementation of algorithms for the validation and prediction of sediments retained inside the reservoir.

3.1. Study Areas and Data Collection

The Indus River is one of the world's greatest rivers, which carries sediments, and supplies the majority of the water that fills Tarbela. The Right Bank tributary of Siran feeds the Indus River upstream of Tarbela, draining an area with a monsoon effect of approximately 6411 kilometers and accounting for only about 6% of the total catchment area. This means that semi-arid to hyper-arid environments make up 94% of the catchment area. At Tarbela, the Indus River drains a catchment area of ~169,644 square kilometers mostly comprising highly denuded barren and glaciated landscapes [4].

The velocity of this water decreases when it enters the Tarbela reservoir, thus reducing its sediment-carrying capacity. So, sediment is deposited there. The sediment coming into Tarbela comprises sand, sediments, and clay. It has been observed that coarse sediments, that is, larger particles, tend to deposit in the upper reaches of the reservoir because they require more velocity of water to be carried with it while fine particles travel toward the dam. So, a sloped shape "delta" is formed in the reservoir. This delta changes its location and expands toward the tunnel intakes as the reservoir is operated over a period of time. Since the reservoir is operated at different water levels for the whole year. The water level varies from high head conditions, that is, July, August, and September when the reservoir is filled, to low head conditions, that is, December, January, February, and March when the reservoir level is decreasing. Every year when the reservoir level reduces, water above this delta erodes the sediment there and carries some quantity along with it. It also deposits some of it near the reservoir, causing the delta to advance toward the tunnel inlets while entraining some of the particles in the flow and carrying the remaining. The sediment carried with water after erosion from the delta can deposit inside the reservoir or can block the tunnel too. In 1997, such an incident took place when suddenly one portal got blocked due to sediments. The cause of that blockage is still not understood, but an event like this may happen again [5]. The location map of the Tarbela Dam and the Reservoir confirmed by the Indus River System Authority, along with the other rivers located near the distance of 200 km, is shown in Figure 2.

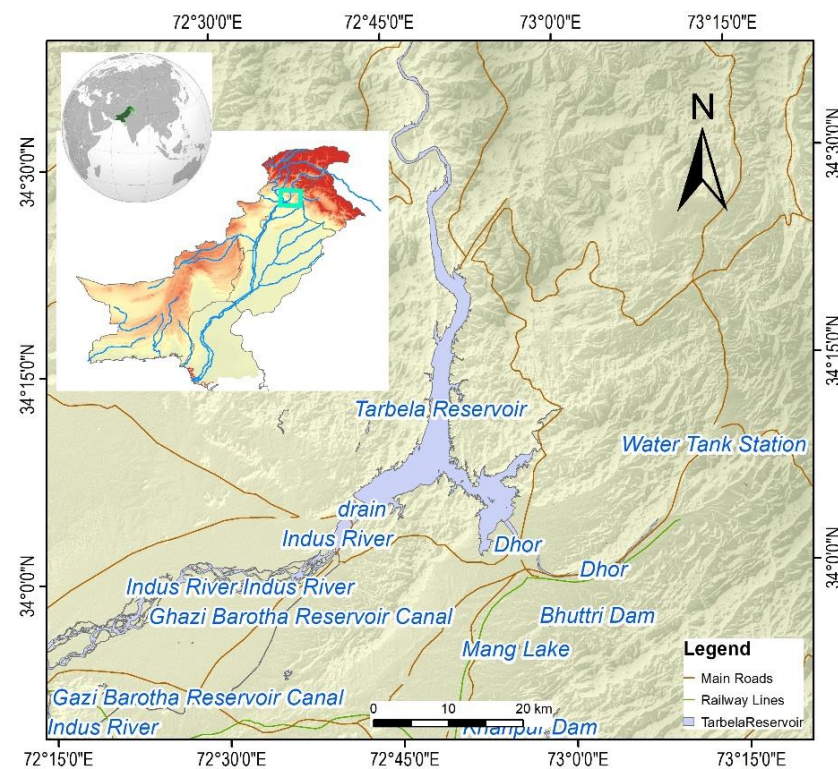


Figure 2. Location map of the Tarbela Dam and the Reservoir confirmed from Indus River System Authority along with the other rivers located near the distance of 200 km.

In addition to yearly rainfall, water inflow, and reservoir storage capacity, minimum reservoir level is also considered an influencing parameter for the analysis performed in this study using data for the years 1985 to 2012. The time series plot of these data in Figure 3 shows the relationship between the reservoir’s rainfall on a yearly basis (R_a), water inflow (I_w), minimum reservoir level (L_r), and reservoir storage capacity (C_r) against the actual sedimentation volume (S_v) deposited inside the Tarbela reservoir shown in blue on the secondary y -axis. The straight lines show the linear trends along with the equations of lines illustrating the relationship between influencing parameters and the actual volume of sedimentation retained inside the Tarbela reservoir. It can be seen that the parameters are correlated, and their regression analysis is performed in the subsequent section.

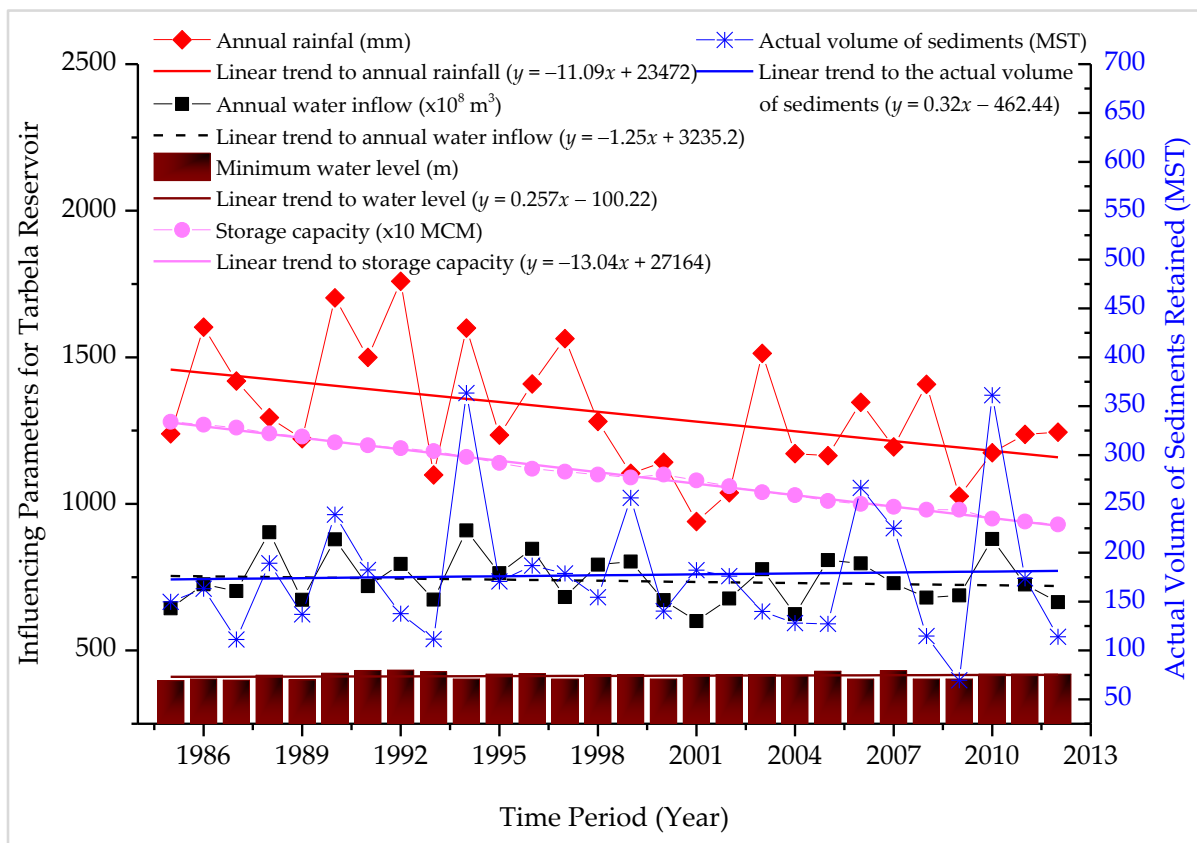


Figure 3. Time series plot of yearly basis influencing parameters including rainfall, water inflow, water level, and the storage capacity of the reservoir used for the estimation of sediments retained inside the Tarbela reservoir from year 1985 to year 2012.

The intricate relationship between the Tarbela reservoir’s sedimentation volume and its inputs was modeled using ANN and multivariate regression. The Tarbela reservoir’s sediment management studies and the yearly sedimentation report of the WAPDA were utilized to gather operational data for the models, which were then used to train the ANN model [4,20].

3.2. Model Development

An ANN consists of small computational elements known as artificial neurons. When arranged in a layered structure form, these neurons are known as multi-layered perceptron artificial neural networks. In ANN, the outer layers are known as input and output layers depending on where we provide our input variables and from where we get our output variables, respectively. The number of neurons in these layers is fixed and dependent on the number of input variables and output variables. Whereas, the layers between the input

layer and the output layer are known as hidden layers and the artificial neurons in these layers are known as hidden neurons. The amount of computation required by an ANN depends on the total number of hidden layers and the number of neurons in each hidden layer. The number of hidden layers and the number of neurons in each hidden layer are used to designate the architecture of neural networks. For example, the N4-45-45-1 ANN structure means that the network has four layers, including one input layer, one output layer, and two hidden layers. It also indicates four neurons in the input layer, 45 neurons in each hidden layer (first and second), and one neuron in the output layer. The typical architecture of the N4-45-45-1 network proposed to predict the sedimentation amount deposited inside the Tarbela reservoir is shown in Figure 4. The hyperparameters used for the optimized neural network are shown in Table 1.

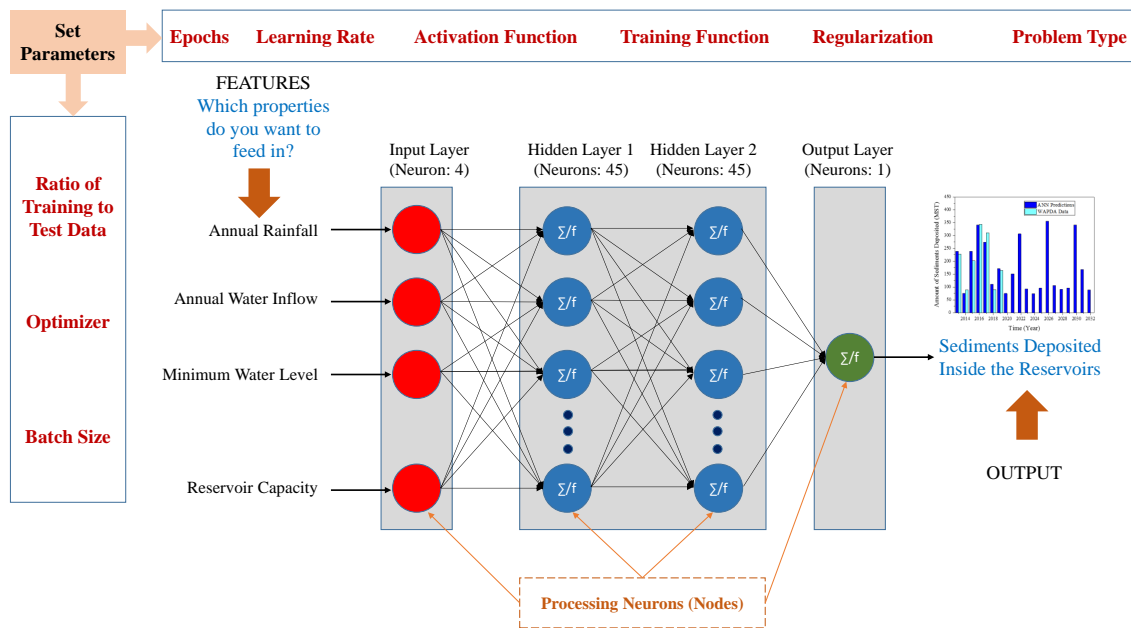


Figure 4. Typical neural network architecture (N4-45-45-1) describing four layers including one input layer, one output layer, and two hidden layers. Four neurons in the input layer, 45 neurons in the first hidden layer, 45 neurons in the second hidden layer, and one neuron in the output layer are also indicated.

Table 1. Hyperparameters of Artificial Neural Network (ANN).

Parameter	Value
Batch size	100
Learning rate	0.001
The number of hidden layers	2
The number of neurons at kth hidden layer	45
The number of neurons at input layer	4
The number of neurons at output layer	1
Activation function	Sigmoid
Training Function	trainrp
Optimizer	Adam
Epoch	20
Regularization	L1 (Lasso regression)
Problem type	Time Series (Sequential)
Ratio of training to test data (%)	82:18

A trial and error method was used to employ the artificial neural network model in MATLAB. The number of hidden layers and the number of neurons in each hidden layer were varied and the most suitable structure that forecasted the results with the least error was chosen. The data normalization between “−1” and “1” was performed using Equation (1) [12].

$$X_{\text{normalized}} = \frac{X - X_{\min}}{X_{\max} - X_{\min}} \tag{1}$$

where X is the data value, X_{\min} is the minimum value in the data, and X_{\max} is the maximum of the data. Equation (2) describes the tangent-sigmoid activation function employed in the neural network models considered in this study. After the first layer, each neuron’s output is estimated using Equation (3).

$$\sigma(x) = \tanh(x) = \frac{2}{1 + e^{-2x}} - 1 \tag{2}$$

$$a^{(i,L)} = \sum \sigma(w^{(i,L)} \times a^{(i,L-1)} + b^{(i,L)}) \tag{3}$$

where $w^{(i,L)}$ is the weight of the i th neuron in the L th layer of the network, $b^{(i,L)}$ represents the bias of the corresponding neuron, and $a^{(i,L-1)}$ represents the signal of the previous layer’s neuron. The activation function is represented by σ .

3.3. Experimental Protocols and Performance Evaluation Measures

The 23 years of data (82% of the total number of data points) were used for the training of the proposed ANN model. For the validation of the proposed neural network model to estimate the Tarbela reservoir sedimentation volume, the following three distinct data sets (each 18% of the total number of data points), shown in Figure 5, were utilized.

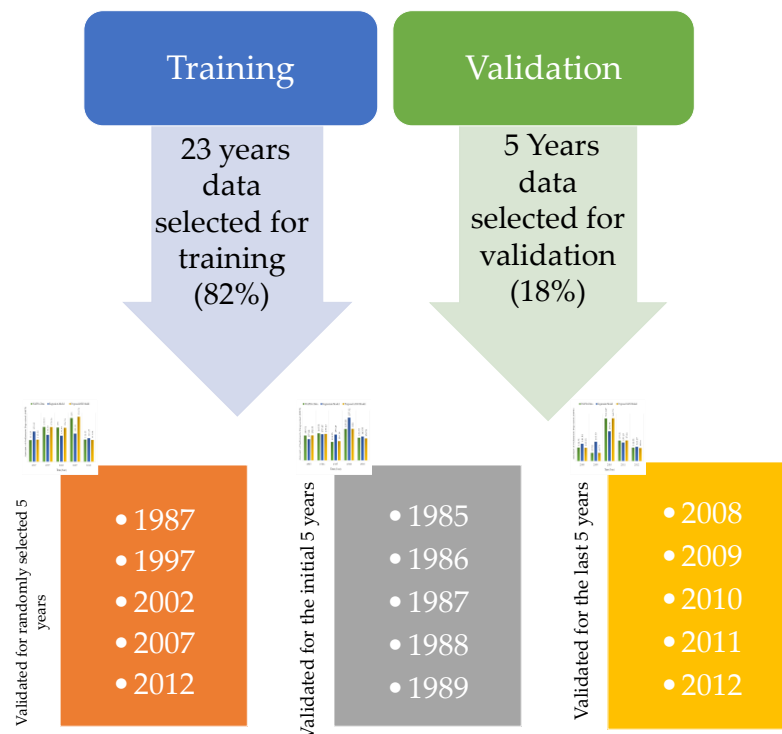


Figure 5. 82% of the data used for training and three different data sets (18% each) used for the validation of trained ANN model considering a randomly selected five-year data set, initial five-year data set, and last five-year data set.

Three different typical neural network architectures $N_{h_i-h_1-h_0}$, $N_{h_i-h_1-h_2-h_0}$, and $N_{h_i-h_1-h_2-h_3-h_0}$ were constructed for training purposes. Where N stands for the ANN architecture, h_i , h_1 , h_2 , h_3 , and h_0 represent the number of neurons in the input layer, in the first hidden layer, in the second hidden layer, in the third hidden layer, and in the output layer, respectively. Different training functions are utilized for the training of proposed neural network architectures.

The training of the neural network was terminated after the MSE with respect to weights and biases reached the respective threshold value, that is, 1×10^{-6} . Based on the prediction value, the exact value (y) supplied using Equation (4), the MSE was determined. Regarding weights and biases, the mean squared error was reduced to a minimum. The biases and weights that were improved were saved for use in later simulations.

$$\text{MSE} = \frac{\sum (a^L - y)^2}{n} \quad (4)$$

Equations (5) and (6) were used to estimate other statistical metrics to check the performance of the model, such as mean absolute error (MAE) and Nash–Sutcliffe efficiency (NSE).

$$\text{MAE} = \frac{\sum |a^L - y|}{n} \quad (5)$$

$$\text{NSE} = 1 - \frac{\sum_1^n (a^L - y)^2}{\sum_1^n (y - \bar{y})^2} \quad (6)$$

where \bar{y} is the mean observed value and a^L is the predicted value. The range of Nash–Sutcliffe efficiency is between - and 1. A perfect match between the predicted and observed data is represented by an NSE value of 1. Equation (7) was used to calculate the relative error.

$$\text{Relative Error} = \frac{|\text{Predicted Value} - \text{Actual Value}|}{\text{Actual Value}} \times 100 \quad (7)$$

4. Results and Discussion

A multivariate regression analysis was conducted to establish a linear relationship between the output and various inputs. A multivariate regression model obtained the slope-intercept form of the relationship between the inputs and the outputs. The regression model, which relates the input with output in slope-intercept, was also used to model sedimentation. The regression was performed using various yearly inputs like rainfall only (R_a), water inflow only (I_w), minimum water level only (L_r), capacity of the reservoir only (C_r), and different combinations of these variables and all variables in multivariate regression. The equations obtained after this regression analysis are given in Table 2.

Figures 6A–D, 7A–D and 8A–D compare the sediment deposition of several multivariate analyses using randomly selected data sets with neural network models employing the same influencing factors. The error bars for the ANN results in these figures are set at a 10% level of uncertainty. Figures 6A–D and 7A–D show that the actual sediment deposition significantly exceeded the error bars for a single input and two inputs, respectively. Figure 8A–C, which displays the results of combining three input parameters, reveals that while ANN model predictions were close to WAPDA data, none of them completely captured the actual data. It is evident that the estimates were most accurate when the water inflow, reservoir storage capacity, and minimum water reservoir level were taken into account. Figure 8D shows that all ANN model estimates fell inside the error bars when rainfall was also considered in these forecasts. The regression model's predictions were still well outside the error bar even though the maximum error for these predictions was 3.01%. To obtain the specific Equation (8b) from the multiple regression analysis, these constants were employed in Equation (8a). Regression analysis demonstrates that the accuracy increases as the number of input parameters increases.

Table 2. Constants evaluated from multivariate regression analysis performed using various yearly basis inputs like rainfall only (R_a), water inflow only (I_w), minimum water level only (L_r), capacity of the reservoir only (C_r), and different combinations of these variables and all variables in multivariate regression.

Variables	p	q	r	s	Intercept
R_a only	0.073212	0	0	0	84.17088
I_w only	0	0.00522	0	0	−218.58
L_r only	0	0	−0.10758	0	224.7589
C_r only	0	0	0	−0.00339	217.077
R_a and I_w	0.00575	−0.04186	0	0	−199.299
I_w and L_r	0	0.005683	−1.32448	0	299.2509
L_r and C_r	0	0	−0.12451	−0.00345	270.0721
I_w and C_r	0	0.005295	0	−0.00513	−162.88
$R_a, I_w,$ and L_r	−0.04103	0.006149	1.3160	0	314.409
$R_a, L_r,$ and C_r	0.0977	0	0.42128	0.01152	354.270
$I_w, L_r,$ and C_r	0	0.005721	1.36206	0.00601	378.5874
All Parameters	−0.033	0.6	−1.34	−0.34	356.96

$$S_v = (p \times R_a) + (q \times I_w) + (r \times L_r) + (s \times C_r) + Intercept \tag{8a}$$

$$S_v = -0.033R_a + 0.6I_w - 1.34L_r + 356.93 \tag{8b}$$

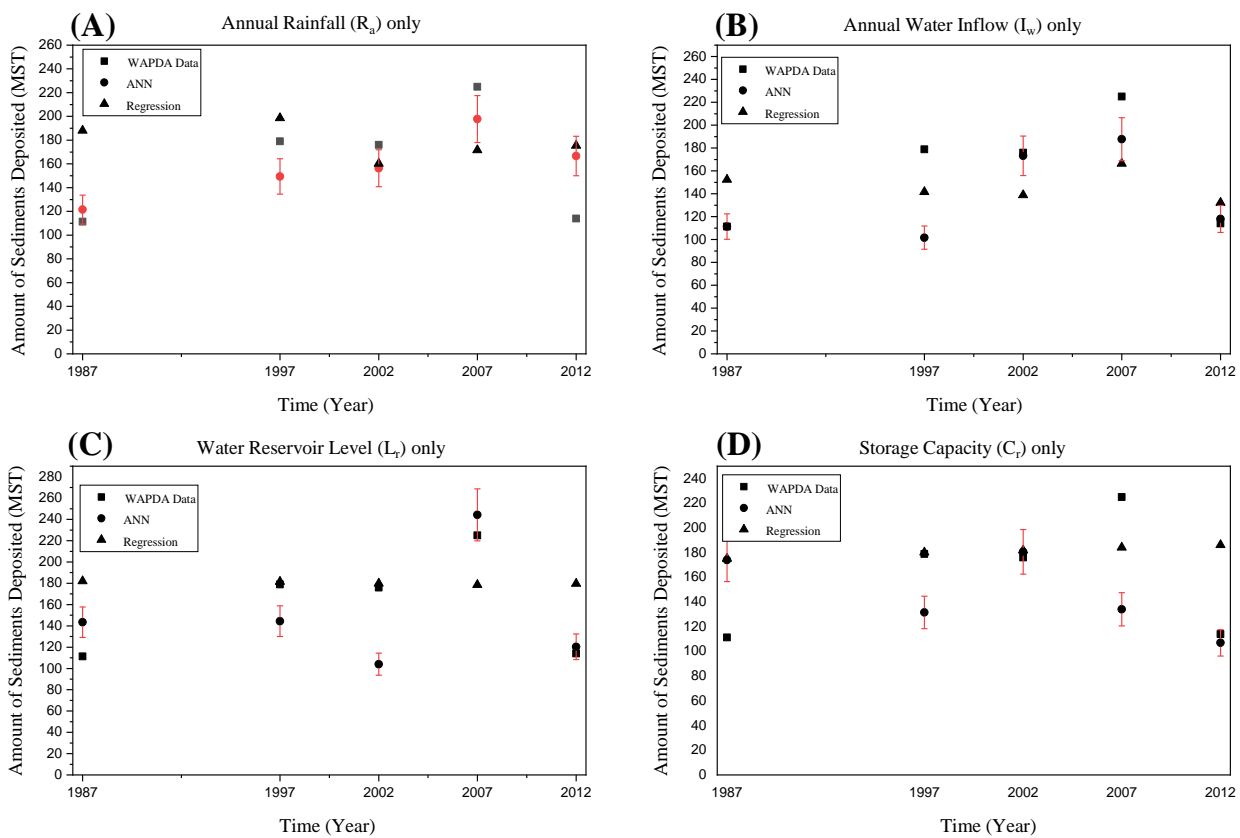


Figure 6. Comparing ANN model with multivariate regression model to calculate the sedimentation amount deposited inside the Tarbela reservoir using only one yearly basis input parameter of (A) rainfall, (B) inflow of water, (C) minimum reservoir level, and (D) storage capacity.

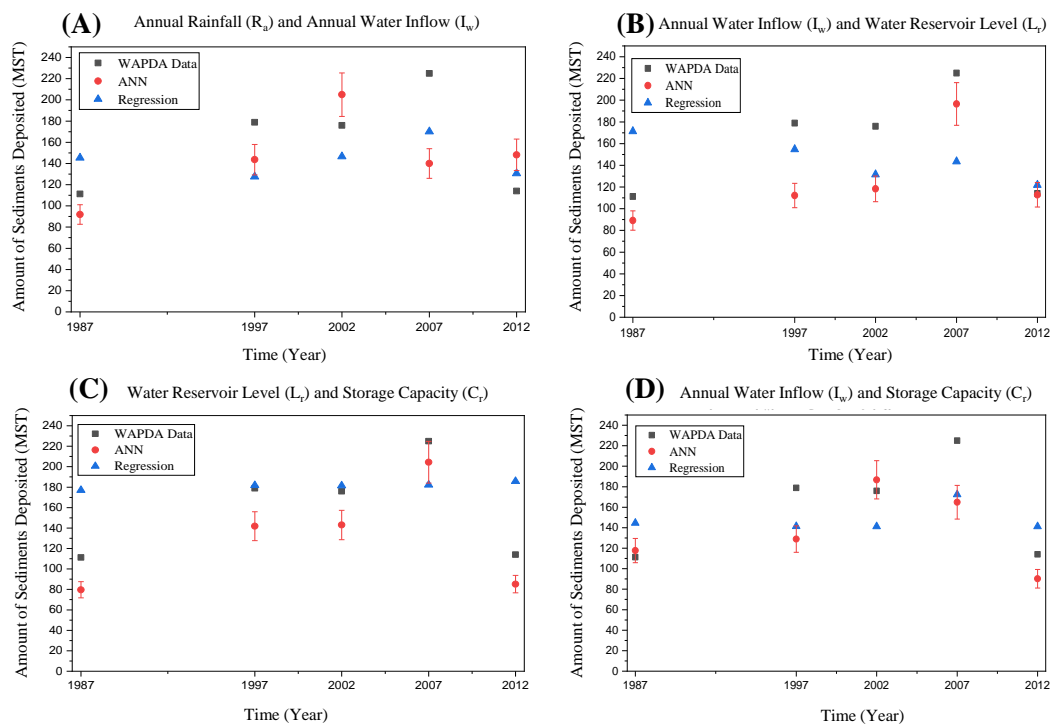


Figure 7. Comparing ANN model with multivariate regression model to compute the amount of sediment in the Tarbela reservoir using only two yearly basis input parameters: (A) rainfall and water inflow; (B) water inflow and minimum reservoir level; (C) minimum reservoir level and storage capacity; and (D) storage capacity and water inflow.

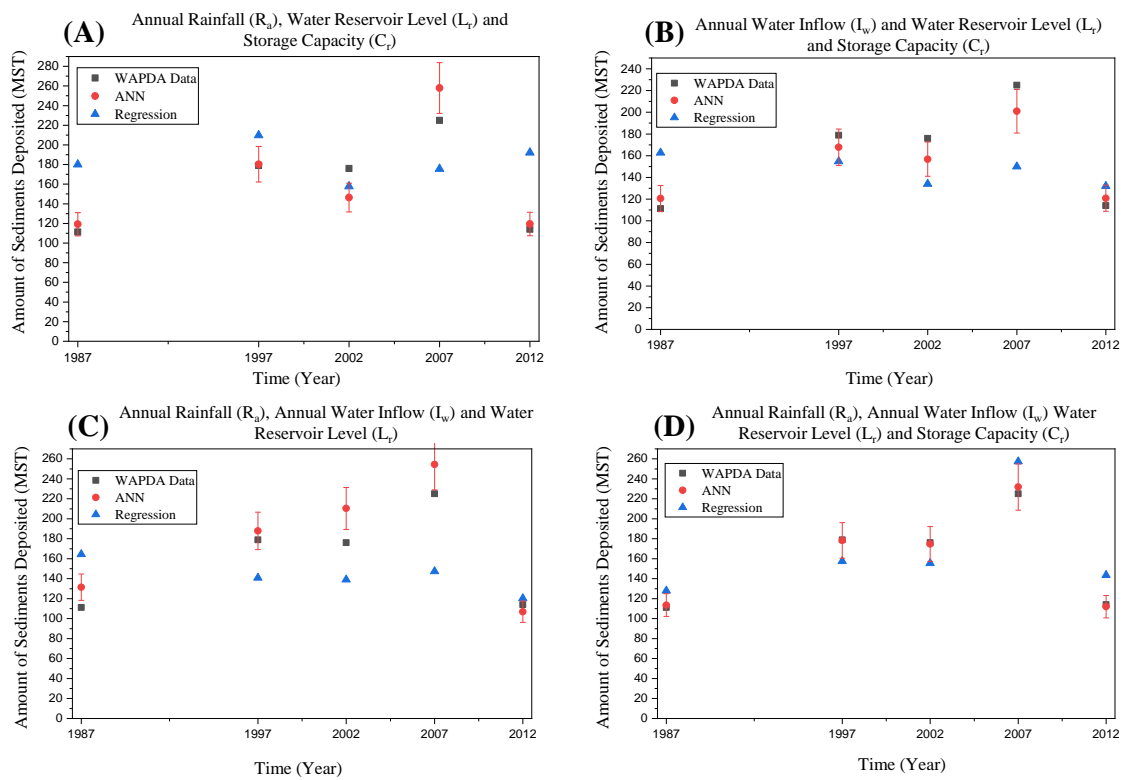


Figure 8. Comparing ANN model with multivariate regression model to compute the Tarbela reservoir sediment deposition with the combination of yearly basis three and four two input parameters:

(A) rainfall, reservoir minimum level, and storage capacity; (B) inflow of water, reservoir minimum level, and reservoir storage capacity; (C) rainfall, inflow of water, and reservoir minimum level; and (D) rainfall, inflow of water, minimum reservoir level, and storage capacity.

For influencing parameters of the data set used for validation, the trained network was simulated. The outcomes of these simulations were compared with the measured values. Based on minimum relative error, the optimal network was chosen. Relative error from Equation (7) was used to evaluate the models' performance.

The relative error of each network for the validation data set is shown in Figure 9. The network N4-45-45-1, which has two hidden layers and 45 neurons in each hidden layer, was shown to have the minimum error for predicting the amount of sediment deposited, with a maximum error of 3.01% for the random data set. The N4-45-45-1 network also tested various training functions. When compared to alternative training functions, it was found that the resilient propagation (RP) accurately predicted the amount of sediment. Figure 10 depicts each training function's percentage inaccuracy. For the random data set, the greatest error in the RP as the training function was observed to be 3.01%.

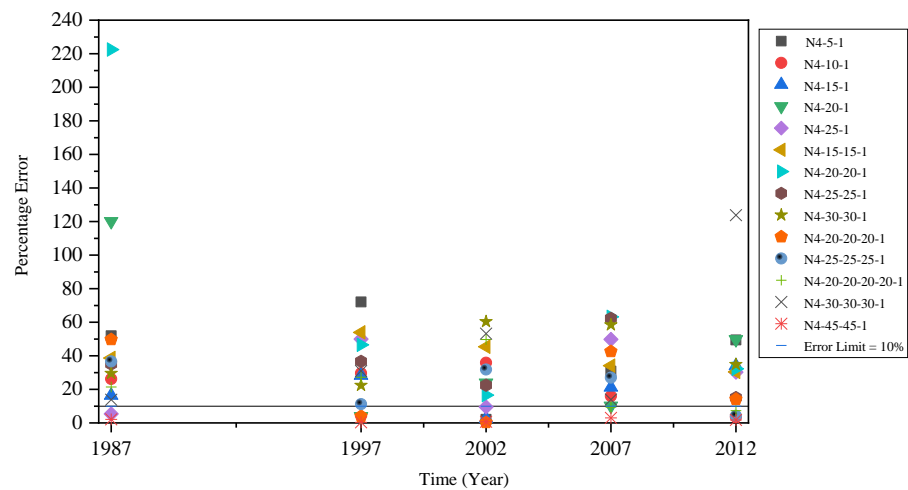


Figure 9. Selection of typical neural network architecture (N4-45-45-1) on the basis of percentage error computed for the validation data set using different ANN architectures.

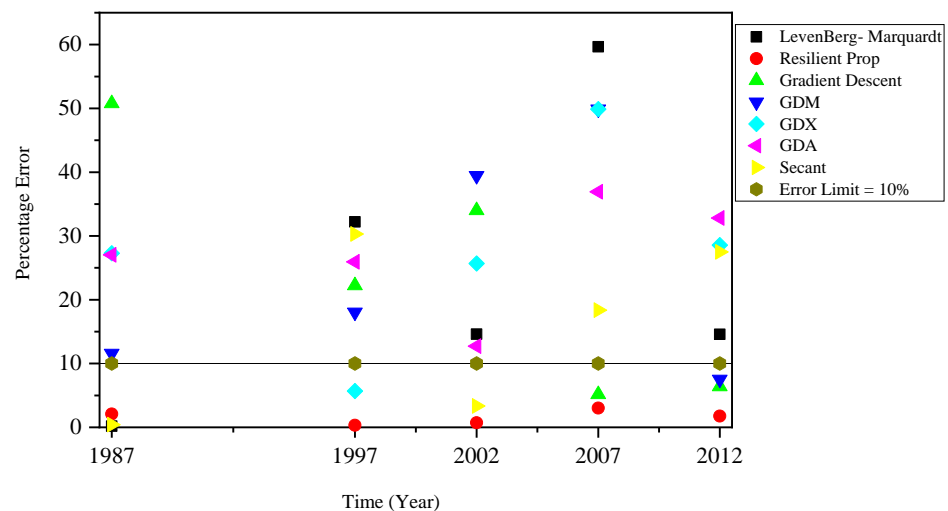


Figure 10. Selection of training function on the basis of percentage error computed for the validation data set using different sets of training functions.

The additional two data sets were then trained for the N4-45-45-1 architecture. It was discovered that any 23 years of data given in this study could be used to train the N4 45-45-1 architecture, and the trained network could successfully predict the data from the remaining years. Table 3 lists the statistical performance indicators for the N4-45-45-1 network for all three data sets, using the resilient propagation as the training function and the tangent sigmoid as the activation function. The proposed neural network architecture accurately predicted the Tarbela reservoir sediment deposition, according to NSE values of 0.99435 for the random data set of 5 years, 0.98721 for the first five years, and 0.99965 for the last five years data set.

Table 3. Performance metrics of the proposed neural network architecture for randomly selected data for 5 years and data selected for first and last 5 years.

Performance Metrics	Randomly Selected 5 Years Data Set	Initial 5 Years Data Set	Last 5 Years Data Set
MSE	0.000529	0.00539	0.000166
MAE	0.017604	0.019629	0.015607
R-Training	0.99928	0.997	1
R-Validation	0.99823	0.991	0.99902
NSE	0.99436	0.98271	0.99965
Minimum Gradient	9.79×10^{-7}	9.18×10^{-7}	9.97×10^{-7}

The Tarbela reservoir's annual sediment deposition is compared in Tables 4–6 using ANN and multivariate regression approaches for the validation data set for the randomly selected data set of 5 years, the initial 5 years, and the last 5 years, respectively. Regression had a maximum inaccuracy of 60.7% when predicting the amount of sediment deposited compared to ANN's 4.41%. Figures 11A, 12A, and 13A show a comparison between the amount of sediment retained inside the Tarbela reservoir obtained by multivariate regression analysis with the proposed ANN model using randomly selected data for the years 1987, 1997, 2002, 2007, and 2012, the initial 5-year data, and last 5-year data respectively. While the bars in Figures 11B, 12B, and 13B show the yearly reduction in relative error of the proposed ANN model in comparison to the reference multivariate regression model for all three training data sets. It can be concluded that the proposed ANN model performs better as compared to the multivariate regression model.

Table 4. Comparison of results obtained by proposed ANN model with the actual amount of sediment quoted by WAPDA and obtained by multiple regression model using the randomly selected data set of 5 years.

Year	Randomly Selected 5 Years Data Set	Initial 5 Years Data Set [R.E. (%)]	Last 5 Years Data Set [R.E. (%)]
1987	111.25	155.45 [39.73]	113.58 [2.10]
1997	178.93	138.39 [22.66]	178.36 [0.32]
2002	176	133.84 [23.95]	174.74 [0.71]
2007	225	144.56 [35.74]	231.76 [3.01]
2012	114.01	121.29 [6.39]	111.98 [1.77]

Table 5. Comparison of results obtained by proposed ANN model with the actual amount of sediment quoted by WAPDA and obtained by multiple regression model using the data set of initial 5 years.

Year	Randomly Selected 5 Years Data Set	Initial 5 Years Data Set [R.E. (%)]	Last 5 Years Data Set [R.E. (%)]
1985	149.72	127.88 [14.59]	150.39 [0.44]
1986	163.21	157.49 [3.5]	159.43 [2.31]

Table 5. *Cont.*

Year	Randomly Selected 5 Years Data Set	Initial 5 Years Data Set [R.E. (%)]	Last 5 Years Data Set [R.E. (%)]
1987	111.25	155.45 [39.73]	116.16 [4.41]
1988	189.28	257.32 [35.94]	190 [0.38]
1989	136.93	143.55 [4.84]	132.56 [3.18]

Table 6. Comparison of results obtained by proposed ANN model with the actual amount of sediment quoted by WAPDA and obtained by multiple regression model using the data set of last 5 years.

Year	WAPDA Data (MST)	Regression Model (MST) [R.E. (%)]	ANN Model (MST) [R.E. (%)]
2008	114.71	146.84 [36.04]	112.95 [1.54]
2009	69.52	163.93 [60.7]	69.71 [0.27]
2010	361.147	252.41 [20.34]	362.75 [0.44]
2011	173.8	157.29 [48.24]	174.6 [0.46]
2012	114.01	121.29 [17.44]	110.6 [2.99]

An approach to graphically summarizing how well a model (or set of patterns) matches data is through the use of Taylor diagrams. The correlation, the centered root-mean-square difference, and the magnitude of the variances between two patterns are used to measure how similar they are (represented by their standard deviations). These diagrams are particularly helpful when comparing the relative abilities of numerous models or when examining multiple facets of complex models. A Taylor diagram is shown in Figure 14 to demonstrate the correlation coefficient, root mean square difference (RMSD), and standard deviation. This figure illustrates how well trends resemble one another and is built using the cosine rule between those three-centered data [75]. On the bottom line, which serves as the reference, a red circle indicates the observation location. Values that are closest to 1 are preferred since the azimuthal axis displays the correlation. Black dashed lines with the standard deviation are used to depict the radial distance from the origin; again, the closer to 1 the better. The lowest distance to the observed location is regarded as the best since it is shown by green dashed lines that depict the root mean square errors as the radial distance from the origin. The proposed ANN model (depicted with a red circle) is shown to have one of the lowest RMSD values and the highest correlation values in the provided Taylor diagram. In addition, its standard deviation is one of the lowest relative to the reference point.

The validation revealed that the proposed neural network model performed better than the regression model, therefore it was applied to forecast how much sedimentation will accumulate inside the Tarbela reservoir during the course of the following 20 years, from 2013 to 2032. By predicting the future data that will be available using the ETS (error, trend, seasonal), a time series univariate forecasting model, the input data for the next 20 years were obtained. With the exception of reservoir storage capacity, there is no overall pattern for the input values, and the ETS model is most appropriate for data without a discernible trend. The four-yearly forecasted input parameters for the Tarbela reservoir including rainfall, water inflow, reservoir minimum level, and storage capacity are shown in Figure 15A–D, respectively. The prediction interval predicts a future individual observation's range. The figure illustrates the lower and upper boundaries of the prediction interval's confidence for the prediction of influencing parameters. The prediction interval is significantly larger, indicating greater uncertainty. The prediction interval expresses the intrinsic uncertainty in the specific data point in addition to the sampling uncertainty. The lower and upper bounds of confidence are set to 95% for predicting all four influencing parameters. Figure 16 shows the forecasts made about how much sediment will be deposited inside the reservoir over the next 20 years. In Figure 16, the forecasts are compared with data from WAPDA for the actual amount of sediment deposited between the years 2013 and 2019. The figure makes it evident that forecasts for this year's sediment deposition are rather close to being accurate.

Comparison of WAPDA Reference Amount of Sediments with Regression and ANN Model using Random Data Set

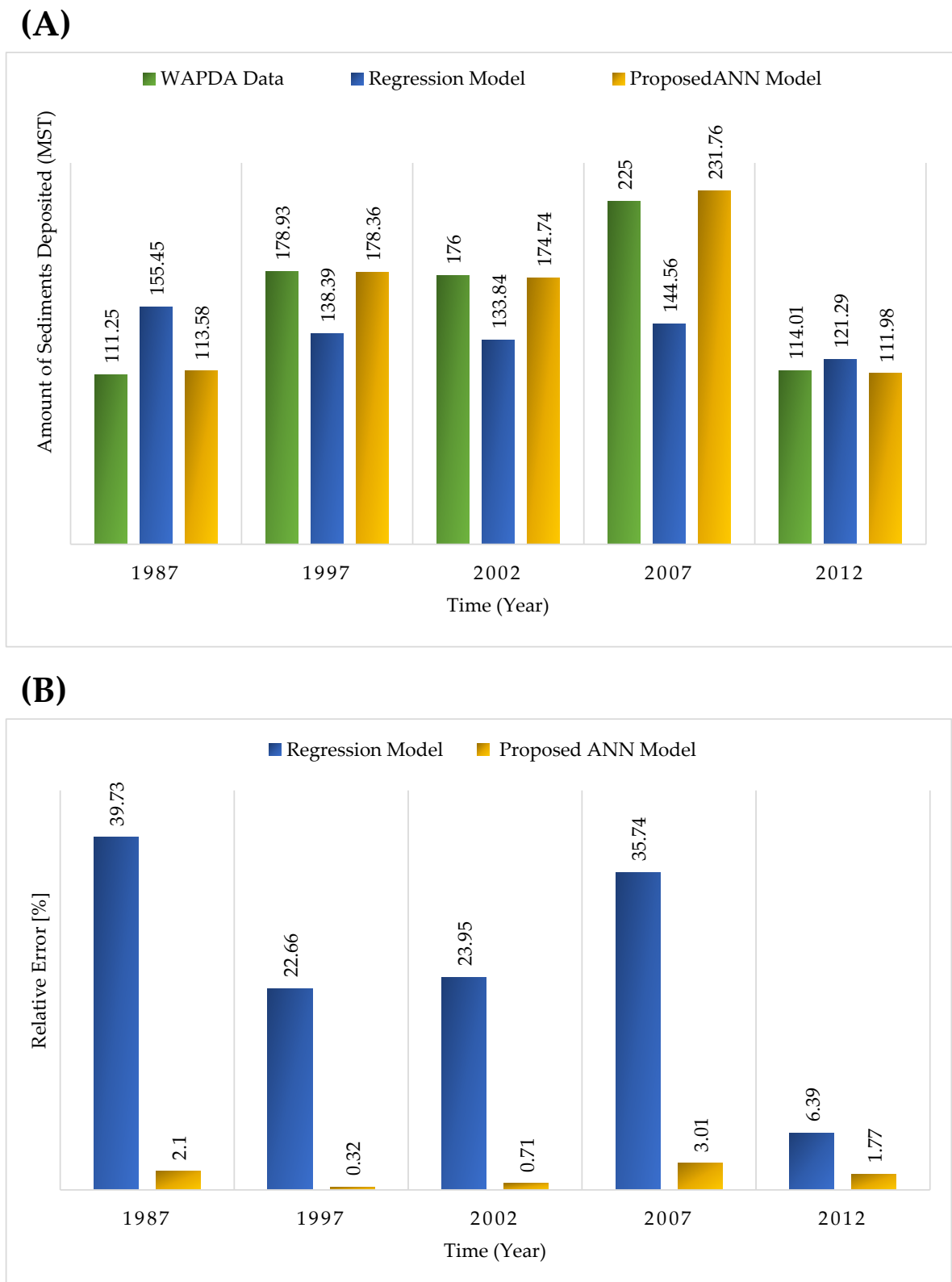


Figure 11. (A) Comparison of actual volume of sediments deposited inside the Tarbela quoted by WAPDA (in green color), obtained by multiple regression model (in blue color) and the proposed ANN model (in gold color) using randomly selected data for 5 years (B) Reduction in relative error of proposed ANN model (in gold color) in comparison with the multiple regression model (in blue color) using randomly selected data for 5 years.

Comparison of WAPDA Reference Amount of Sediments with Regression and ANN Model using Initial 5 Years Data Set

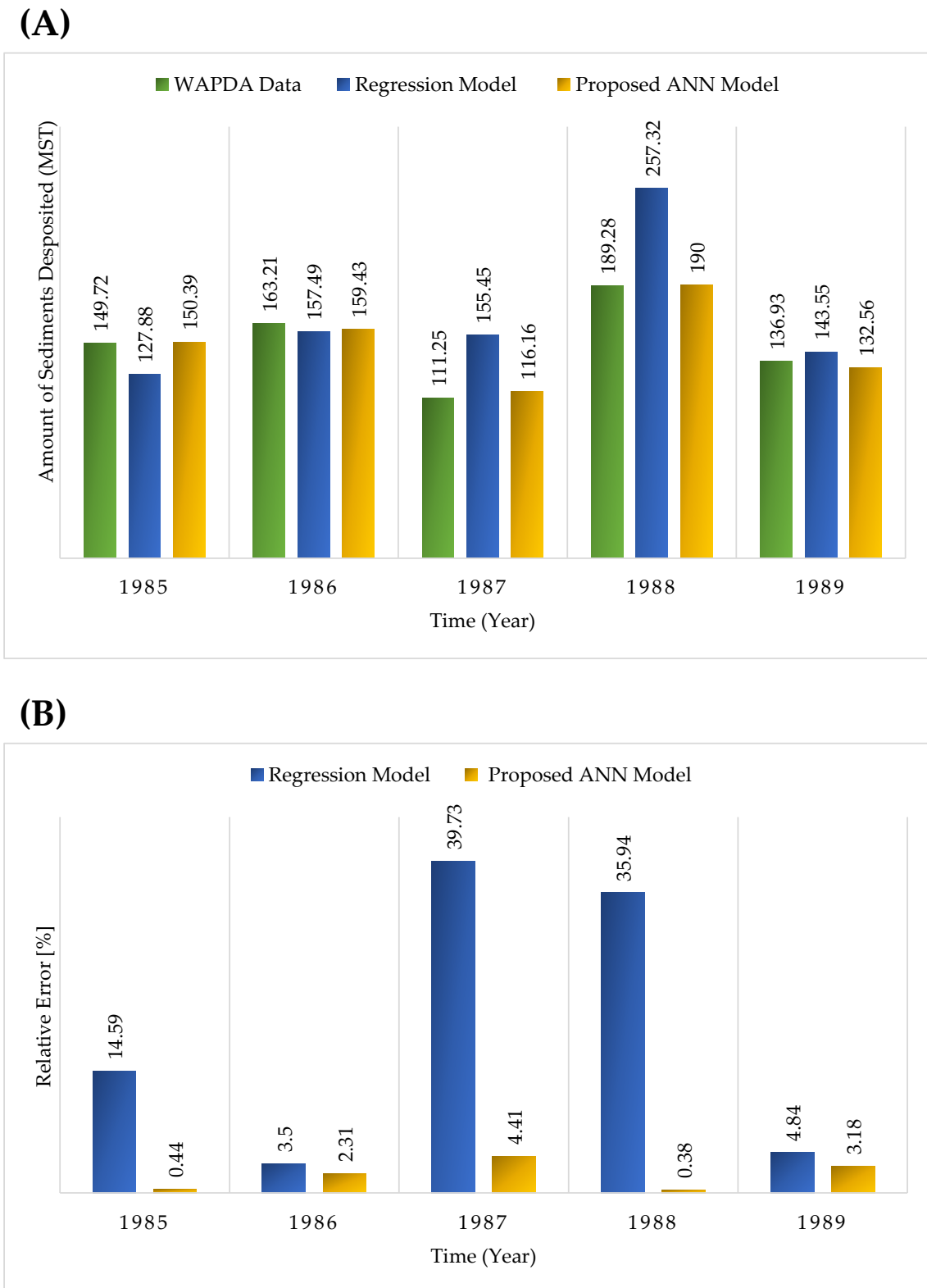


Figure 12. (A) Comparison of actual volume of sediments deposited inside the Tarbela quoted by WAPDA (in green color), obtained by multiple regression model (in blue color) and the proposed ANN model (in gold color) using data for initial 5 years (B) Reduction in relative error of proposed ANN model (in gold color) in comparison with the multiple regression model (in blue color) using data for initial 5 years.

Comparison of WAPDA Reference Amount of Sediments with Regression and ANN Model using Last 5 Years Data Set

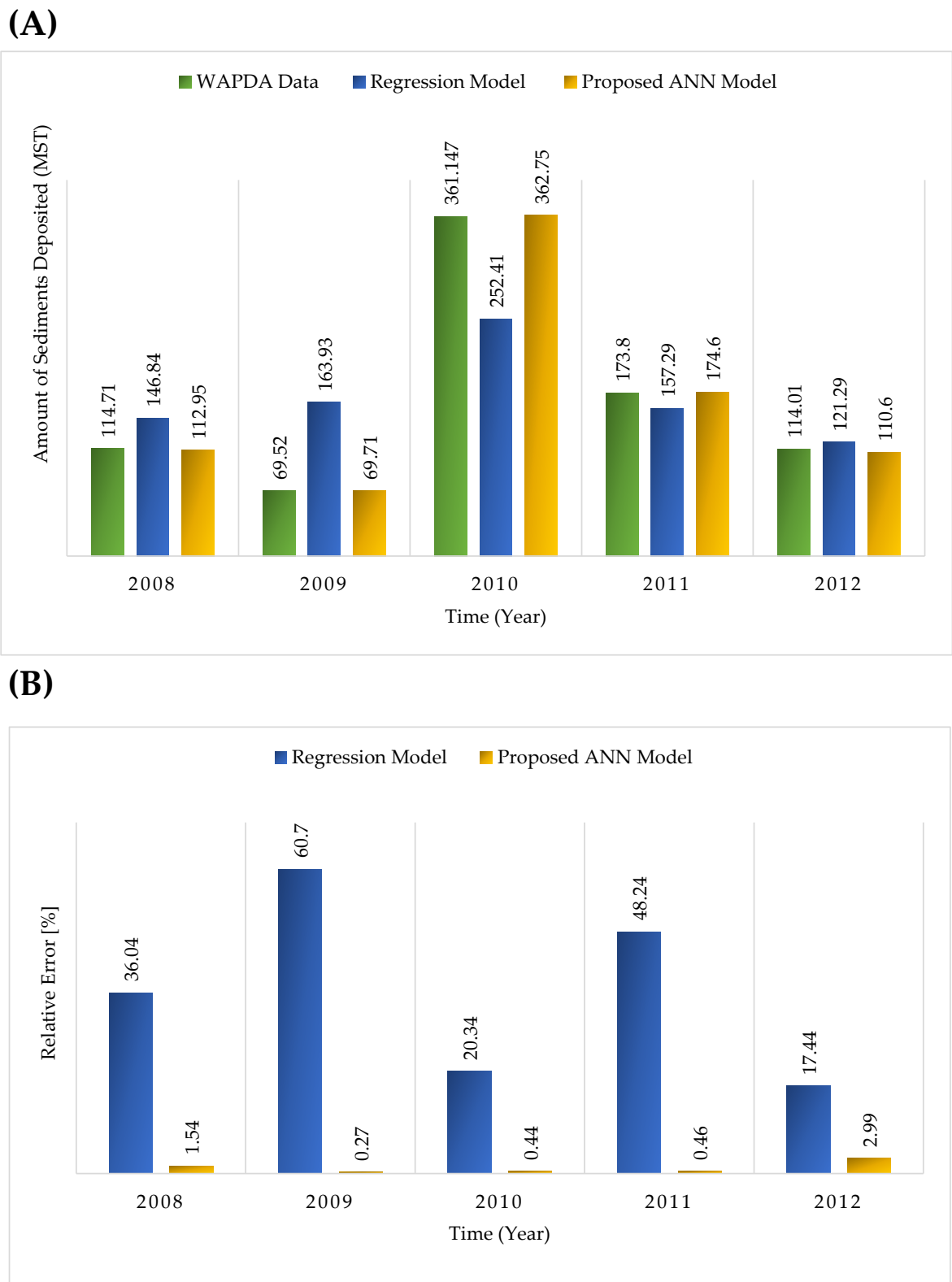


Figure 13. (A) Comparison of actual volume of sediments deposited inside the Tarbela quoted by WAPDA (in green color), obtained by multiple regression model (in blue color) and the proposed ANN model (in gold color) using data for last 5 years (B) Reduction in relative error of proposed ANN model (in gold color) in comparison with the multiple regression model (in blue color) using data for last 5 years.

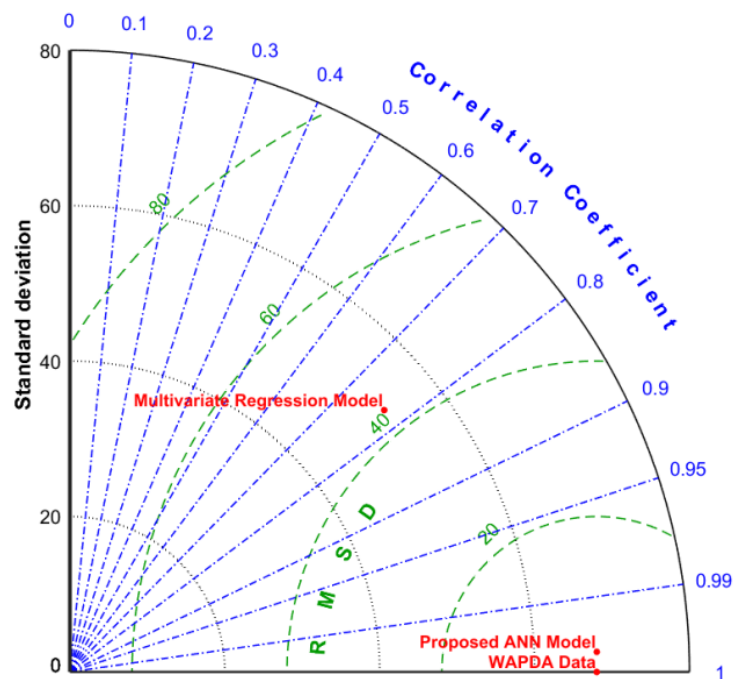


Figure 14. Taylor Diagram for the evaluation of model performance, where blue dotted lines show the Pearson’s correlation coefficient (R), black dotted arcs represent the standard deviation and green dashed arcs show the root mean squared difference. Red dots show which model is closer to the reference WAPDA data and performing better.

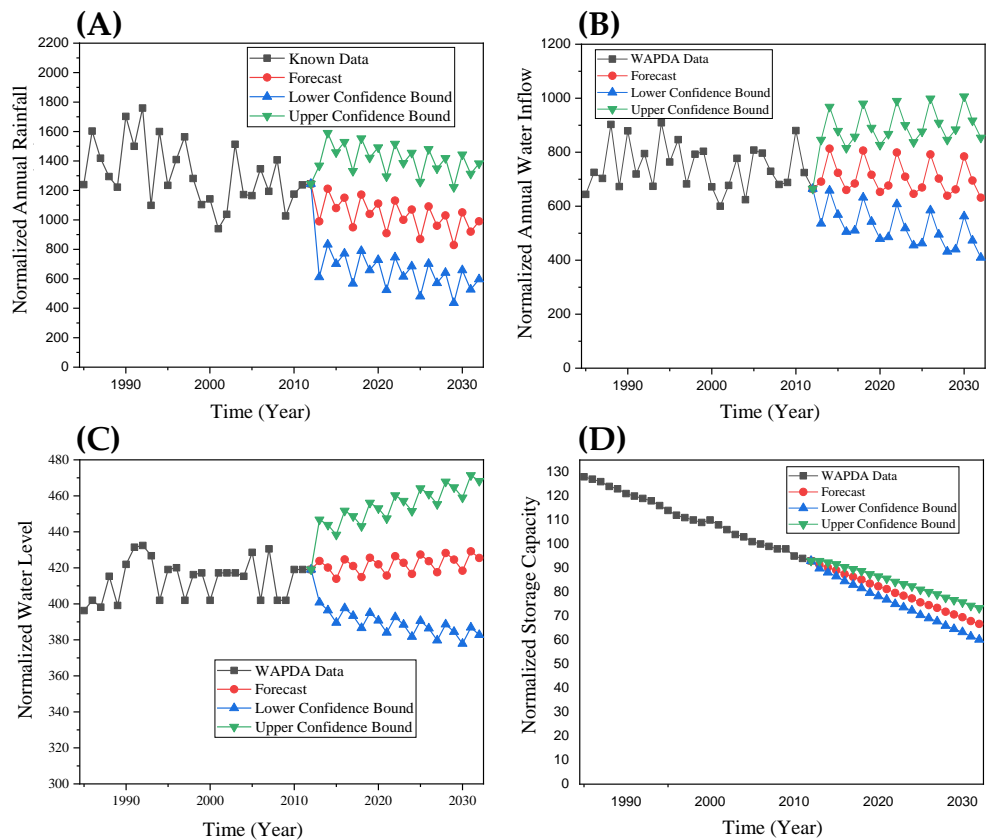


Figure 15. Forecasting of yearly basis influential factors for the Tarbela reservoir: (A) normalized values of rainfall; (B) normalized inflow of water; (C) normalized minimum level of reservoir; (D) normalized storage capacity.

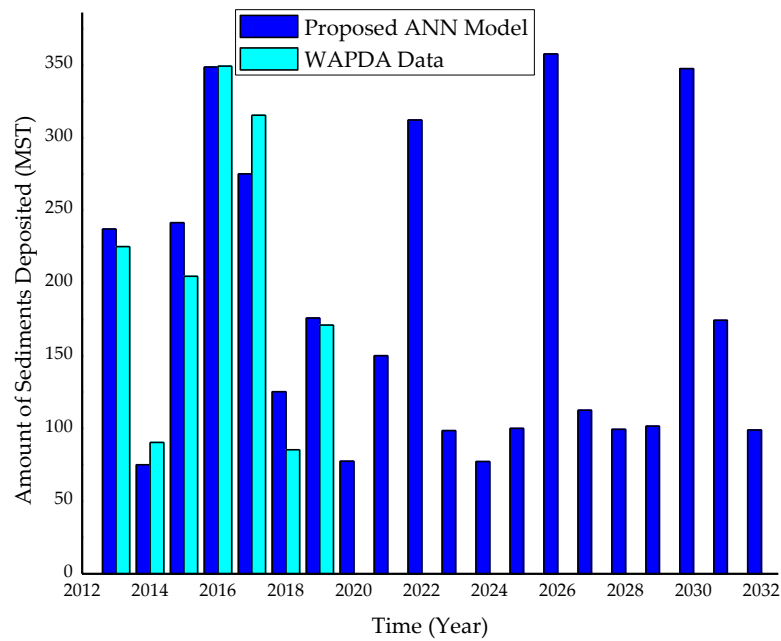


Figure 16. Sedimentation prediction for next 20 years using proposed ANN model based on the four forecasted input parameters for the Tarbela reservoir.

The relative significance of each influencing factor in estimating the sediment deposition inside the Tarbela reservoir was evaluated using the method proposed by Olden et al. [76]. The connection weight strategy was shown to be the only approach that consistently determined the correctly ranked importance of all predictor variables, according to a comparison by Olden et al. and many other techniques for evaluating the relative importance of each parameter in ANN. In Figure 17, the storage capacity of the reservoir was shown to be the most important influencing factor in estimating the amount of sediment deposited, whilst annual rainfall was found to be less important.

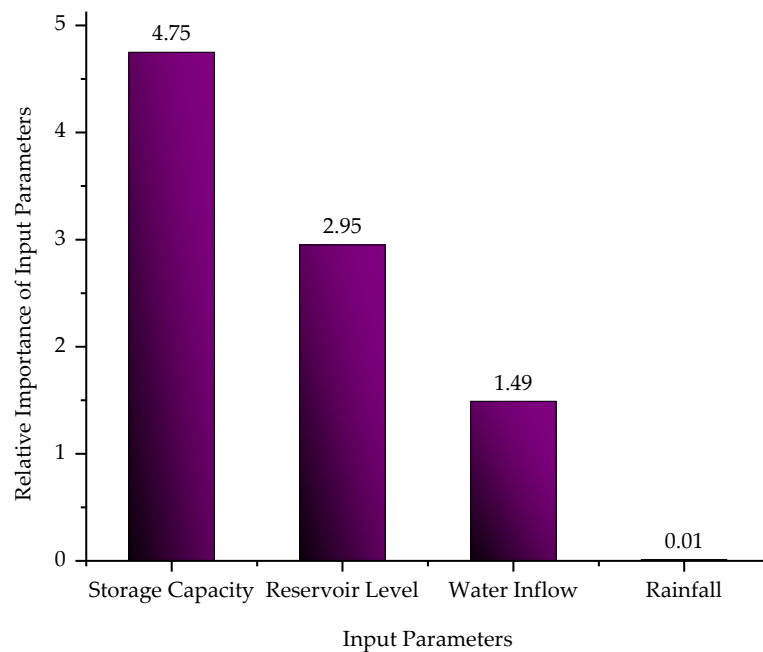


Figure 17. The relative significance of influencing parameters in predicting the sedimentation amount deposited inside the Tarbela reservoir assessed using Olden’s algorithm of connection weights.

5. Conclusions

This study employed an artificial neural network and multivariate regression techniques to predict the annual sediment deposition inside the Tarbela reservoir in Pakistan. Firstly, multivariate regression analysis was performed using various combinations of yearly basis four influencing parameters, including rainfall (R_a), water inflow (I_w), minimum level of reservoir (L_r), and storage capacity of the reservoir (C_r). It was determined that with the increase in the number of influencing parameters, the accuracy of the sediment deposition prediction is increased. Secondly, different neural network architectures with various training functions were employed. It was found that the typical N4-45-45-1 neural network architecture with the resilient propagation training function performs better with a minimum error of 3.01% compared to all other architectures and training functions. The proposed neural network model was then applied for validation and future prediction purposes. It was found that the four influencing parameters could be used to accurately estimate the amount of sediment deposited inside the Tarbela reservoir. The maximum error for the proposed neural network model was found to be 4.01%, whereas, in the case of the multivariate regression model, it was found to be 60.7%, leading to the conclusion that the proposed neural network model approximated the amount of sediment deposited more accurately than the multivariate regression model. Finally, the Tarbela reservoir's sedimentation was predicted using forecasted data of 20 years for four input parameters from the ETS model. It was found that the predictions are in good agreement with the actual sediment deposition determined by WAPDA for the years 2013 to 2019. It was also concluded using Olden's technique that the Tarbela's storage capacity is the most important influencing parameter in determining the amount of sedimentation inside of it, whilst annual rainfall was found to be less significant in influencing the amount of sediment deposited.

Standalone machine learning approaches like ANN can accurately predict the amount of sediment in reservoirs compared to traditional multiple regression approaches. However, some other conventional models (e.g., KNN, SVM, DT, RF, XGBoost) can also be implemented for the same problem in future research and can be compared with the ANN to demonstrate how different models are performing. Despite its ability to predict sediment volume, standalone machine learning approaches have several limitations that should be highlighted. In general, hybrid ML models should be developed as well, which are more accurate and reliable than independent ML models.

Author Contributions: Conceptualization, N.S. and M.A.; methodology, S.H. and N.S.; software, S.H., A.H., A.A.; validation, S.H., N.S. and M.A.U.R.T.; formal analysis, S.H. and Z.R.; investigation, M.L.U.R.S. and M.A.U.R.T.; resources, M.A.U.R.T.; data curation, N.S. and Z.R.; writing—original draft preparation, N.S. and S.H.; writing—review and editing, N.S., M.A.U.R.T., A.H., M.A.; visualization, N.S., S.H.; supervision, N.S., M.A., M.L.U.R.S. and M.A.U.R.T.; project administration, M.A.U.R.T.; funding acquisition, M.A.U.R.T. All authors have read and agreed to the published version of the manuscript.

Funding: This research received no external funding.

Data Availability Statement: Not applicable.

Acknowledgments: The authors acknowledge the efforts of the Water and Power Development Authority (WAPDA) of Pakistan for providing the necessary data required for this study.

Conflicts of Interest: The authors declare no conflict of interest.

Nomenclature

The following abbreviations are used in this manuscript:

ANN	Artificial Neural Network
ETS	Error, Trend, Seasonal
MT	Million Tonnes
MST	Million Short Tons
MSE	Mean Squared Error
MAE	Mean Absolute Error
NSE	Nash–Sutcliffe Efficiency
R_a	Annual rainfall
I_w	Water inflow annually
L_R	The minimum water level in the reservoir
C_r	Capacity of reservoir
S_R	Amount of sediment deposited annually
$N_{h_i-h_1-h_0}$	N stands for ANN architecture, h_i = number of neurons in the input layer h_1 = number of neurons in the hidden layer h_0 = number of neurons in the output layer
$N_{h_i-h_1-h_2-h_0}$	N stands for ANN architecture, h_i = number of neurons in the input layer h_1 = number of neurons in the first hidden layer h_2 = number of neurons in the second hidden layer h_0 = number of neurons in the output layer
$N_{h_i-h_1-h_2-h_3-h_0}$	N stands for ANN architecture, h_i = number of neurons in the input layer h_1 = number of neurons in the first hidden layer h_2 = number of neurons in the second hidden layer h_3 = number of neurons in the third hidden layer h_0 = number of neurons in the output layer
R	Correlation Coefficient
R.E.	Relative Error

References

1. Pritchard, S. Overloaded-International Water Power Dam Construction. *Progress. Media Int.* **2002**, *54*, 18–22.
2. Abid, M.; Muftooh, U.R.; Adnan, A.N. *Water and Sediment Flow Simulations for Tarbela Reservoir and Tunnels, a Preliminary Study*. VDM Verlag Dr. Muler. printed in the U.S.A. and in the U.K. 2011. Available online: <https://www.amazon.com/Sediment-Simulations-Tarbela-Reservoir-Tunnels/dp/363934183X> (accessed on 1 August 2022).
3. Abid, M.; Muftooh, U.R.S. Multiphase Flow Simulations through Tarbela Dam Spillways and Tunnels. *J. Water Resour. Prot.* **2010**, *2*, 532–539. [[CrossRef](#)]
4. Water and Power Development Authority (WAPDA). *Tarbela Reservoir Sedimentation Report*; WAPDA: Lahore, Pakistan, 2019.
5. Consultants, Ghazi–Garriala Hydropower (G.G.H). *Technical Report No. 3, Sedimentology of Ghazi-Garriala Hydropower Project, Feasibility Report*; Water & Power Development Authority: Lahore, Pakistan, 1991.
6. Consultants, D.B. *Reservoir Sedimentation Studies, Appendix C to Reservoir Operation and Sediment Transport*; Water and Power Development Authority: Pakistan, Lahore, 2007.
7. Roca, M. Tarbela Dam in Pakistan. Case Study of Reservoir Sedimentation. In Proceedings of the River Flow, San José, Costa Rica, 5–7 September 2012. Available online: <http://eprints.hrwallingford.com/id/eprint/891> (accessed on 15 August 2022).
8. Abrahath, R.J.; White, S.M. Modelling sediment transfer in Malawi: Comparing backpropagation neural network solutions against a multiple linear regression benchmark using small data sets. *Phys. Chem. Earth Part B Hydrol. Ocean. Atmos.* **2001**, *26*, 19–24. [[CrossRef](#)]
9. Cigizoglu, H.K. Suspended Sediment Estimation and Forecasting using Artificial Neural Networks. *Turkish J. Eng. Env. Sci.* **2002**, *26*, 15–25.
10. Cigizoglu, H.K. Suspended Sediment Estimation for Rivers using Artificial Neural Networks and Sediment Rating Curves. *Turkish J. Eng. Env. Sci.* **2002**, *26*, 27–36.
11. Dibike, Y.B.; Solomatine, D.; Abbott, M.B. On encapsulation of numeric–hydraulic models in artificial neural networks. *J. Hyd. Res.* **2010**, *37*, 147–161. [[CrossRef](#)]

12. Li, X.; Qiu, J.; Shang, Q.; Li, F. Simulation of Reservoir Sediment Flushing of the Three Gorges Reservoir Using an Artificial Neural Network. *Appl. Sci.* **2016**, *6*, 148. [[CrossRef](#)]
13. Tarar, Z.R.; Ahmad, S.R.; Ahmad, I.; Hasson, S.U.; Khan, Z.M.; Washakh, R.M.A.; Ateeq-Ur-Rehman, S.; Bui, M.D. Effect of Sediment Load Boundary Conditions in Predicting Sediment Delta of Tarbela Reservoir in Pakistan. *Water* **2019**, *11*, 1716. [[CrossRef](#)]
14. Rashid, M.U.; Shakir, A.S.; Khan, N.M. Evaluation of Sediment Management Options and Minimum Operation Levels for Tarbela Reservoir, Pakistan. *Arabian J. Sci. Eng.* **2014**, *39*, 2655–2668. [[CrossRef](#)]
15. Petkovsek, G.; Roca, M. Impact of Reservoir Operation on Sediment Deposition. Proceedings of ICE-Water Management. *Thomas Telford Ltd.* **2014**, *167*, 577–584. [[CrossRef](#)]
16. Khan, N.M.; Tingsanchali, T. Optimization and simulation of reservoir operation with sediment evacuation: A case study of the Tarbela Dam, Pakistan. *Hydrol. Proc.* **2009**, *23*, 730–747. [[CrossRef](#)]
17. Arfan, M.; Lund, J.; Hassan, D.; Saleem, M.; Ahmad, A. Assessment of Spatial and Temporal Flow Variability of the Indus River. *Resources* **2019**, *8*, 103. [[CrossRef](#)]
18. Ul Hussan, W.; Khurram Shahzad, M.; Seidel, F.; Costa, A.; Nestmann, F. Comparative Assessment of Spatial Variability and Trends of Flows and Sediments under the Impact of Climate Change in the Upper Indus Basin. *Water* **2020**, *12*, 730. [[CrossRef](#)]
19. Chiang, Y.M.; Chang, L.C.; Chang, F.J. Comparison of static-feedforward and dynamic-feedback neural networks for rainfall-runoff modeling. *J. Hydr.* **2004**, *290*, 297–311. [[CrossRef](#)]
20. Attewill, L.J.S.; White, W.R.; Tariq, S.M.; Bilgi, A. Sediment management studies of Tarbela dam, Pakistan. In *The prospect for reservoirs in the 21st century, Proceedings of the 10th Conference of the British Dam Society, Bangor, UK, 9–12 September 1998*; Thomas Telford Publishing: London, UK, 1998; pp. 212–225.
21. Axel, R.; Rafael, M.C. Performance evaluation of hydrological models: Statistical significance for reducing subjectivity in goodness-of-fit assessments. *J. Hydrol.* **2013**, *480*, 33–45. [[CrossRef](#)]
22. Gusarov, A.V.; Sharifullin, A.G.; Beylich, A.A. Contemporary Trends in River Flow, Suspended Sediment Load, and Soil/Gully Erosion in the South of the Boreal Forest Zone of European Russia: The Vyatka River Basin. *Water* **2021**, *13*, 2567. [[CrossRef](#)]
23. Török, G.T.; Baranya, S.; Rütther, N. 3D CFD Modeling of Local Scouring, Bed Armoring and Sediment Deposition. *Water* **2017**, *9*, 56. [[CrossRef](#)]
24. Rodríguez-Blanco, M.L.; Arias, R.; Taboada-Castro, M.M.; Nunes, J.P.; Keizer, J.J.; Taboada-Castro, M.T. Potential Impact of Climate Change on Suspended Sediment Yield in NW Spain: A Case Study on the Corbeira Catchment. *Water* **2016**, *8*, 444. [[CrossRef](#)]
25. Di Francesco, S.; Biscarini, C.; Manciola, P. Characterization of a Flood Event through a Sediment Analysis: The Tescio River Case Study. *Water* **2016**, *8*, 308. [[CrossRef](#)]
26. Xiao, L.; Yang, X.; Cai, H. Responses of Sediment Yield to Vegetation Cover Changes in the Poyang Lake Drainage Area, China. *Water* **2016**, *8*, 114. [[CrossRef](#)]
27. Yang, X.; Mao, Z.; Huang, H.; Zhu, Q. Using GOCI Retrieval Data to Initialize and Validate a Sediment Transport Model for Monitoring Diurnal Variation of SSC in Hangzhou Bay, China. *Water* **2016**, *8*, 108. [[CrossRef](#)]
28. Tfwala, S.S.; Wang, Y.-M. Estimating Sediment Discharge Using Sediment Rating Curves and Artificial Neural Networks in the Shiwen River, Taiwan. *Water* **2016**, *8*, 53. [[CrossRef](#)]
29. Guerrero, M.; Rütther, N.; Szupiany, R.; Haun, S.; Baranya, S.; Latosinski, F. The Acoustic Properties of Suspended Sediment in Large Rivers: Consequences on ADCP Methods Applicability. *Water* **2016**, *8*, 13. [[CrossRef](#)]
30. Yin, D.; Xue, Z.G.; Gochis, D.J.; Yu, W.; Morales, M.; Rafieeiniasab, A. A Process-Based, Fully Distributed Soil Erosion and Sediment Transport Model for WRF-Hydro. *Water* **2020**, *12*, 1840. [[CrossRef](#)]
31. Nabi, G.; Hussain, F.; Wu, R.-S.; Nangia, V.; Bibi, R. Micro-Watershed Management for Erosion Control Using Soil and Water Conservation Structures and SWAT Modeling. *Water* **2020**, *12*, 1439. [[CrossRef](#)]
32. Némětová, Z.; Honek, D.; Kohnová, S.; Hlavčová, K.; Šulc Michalková, M.; Sočuvka, V.; Velísková, Y. Validation of the EROSION-3D Model through Measured Bathymetric Sediments. *Water* **2020**, *12*, 1082. [[CrossRef](#)]
33. Luffman, I.; Nandi, A. Seasonal Precipitation Variability and Gully Erosion in Southeastern USA. *Water* **2020**, *12*, 925. [[CrossRef](#)]
34. Tavelli, M.; Piccolroaz, S.; Stradiotti, G.; Pisaturo, G.R.; Righetti, M. A New Mass-Conservative, Two-Dimensional, Semi-Implicit Numerical Scheme for the Solution of the Navier-Stokes Equations in Gravel Bed Rivers with Erodible Fine Sediments. *Water* **2020**, *12*, 690. [[CrossRef](#)]
35. Kaffas, K.; Saridakis, M.; Spiliotis, M.; Hrissanthou, V.; Righetti, M. A Fuzzy Transformation of the Classic Stream Sediment Transport Formula of Yang. *Water* **2020**, *12*, 257. [[CrossRef](#)]
36. Xin, Y.; Xie, Y.; Liu, Y. Effects of Residue Cover on Infiltration Process of the Black Soil under Rainfall Simulations. *Water* **2019**, *11*, 2593. [[CrossRef](#)]
37. Al Sayah, M.J.; Nedjai, R.; Kaffas, K.; Abdallah, C.; Khouri, M. Assessing the Impact of Man-Made Ponds on Soil Erosion and Sediment Transport in Limnological Basins. *Water* **2019**, *11*, 2526. [[CrossRef](#)]
38. Wang, G.; Tian, S.; Hu, B.; Xu, Z.; Chen, J.; Kong, X. Evolution Pattern of Tailings Flow from Dam Failure and the Buffering Effect of Debris Blocking Dams. *Water* **2019**, *11*, 2388. [[CrossRef](#)]
39. Lu, C.M.; Chiang, L.C. Assessment of Sediment Transport Functions with the Modified SWAT-Twn Model for a Taiwanese Small Mountainous Watershed. *Water* **2019**, *11*, 1749. [[CrossRef](#)]

40. Song, Y.H.; Yun, R.; Lee, E.H.; Lee, J.H. Predicting Sedimentation in Urban Sewer Conduits. *Water* **2018**, *10*, 462. [CrossRef]
41. Aksoy, H.; Mahe, G.; Meddi, M. Modeling and Practice of Erosion and Sediment Transport under Change. *Water* **2019**, *11*, 1665. [CrossRef]
42. Hauer, C. Sediment Management: Hydropower Improvement and Habitat Evaluation. *Water* **2020**, *12*, 3470. [CrossRef]
43. Patil, M.P.; Jeong, I.; Woo, H.-E.; Oh, S.-J.; Kim, H.C.; Kim, K.; Nakashita, S.; Kim, K. Effect of Bacillus subtilis Zeolite Used for Sediment Remediation on Sulfide, Phosphate, and Nitrogen Control in a Microcosm. *Int. J. Environ. Res. Public Health* **2022**, *19*, 4163. [CrossRef] [PubMed]
44. Reisenbüchler, M.; Bui, M.D.; Skublics, D.; Rutschmann, P. Sediment Management at Run-of-River Reservoirs Using Numerical Modelling. *Water* **2020**, *12*, 249. [CrossRef]
45. Sotiri, K.; Hilgert, S.; Duraes, M.; Armino, R.A.; Wolf, N.; Scheer, M.B.; Kishi, R.; Pakzad, K.; Fuchs, S. To What Extent Can a Sediment Yield Model Be Trusted? A Case Study from the Passaúna Catchment. Brazil. *Water* **2021**, *13*, 1045. [CrossRef]
46. Jothiprakash, V.; Garg, V. Reservoir Sedimentation Estimation Using Artificial Neural Network. *J. Hydrol. Eng.* **2009**, *14*, 1035–1040. [CrossRef]
47. Chen, S.L.; Zhang, G.A.; Young, S.L.; Shi, J.Z. Temporal variations of fine suspended sediment concentration in the Changjiang River estuary and adjacent coastal waters, China. *J. Hydrol.* **2006**, *331*, 137–145. [CrossRef]
48. Wang, Y.M.; Tfwala, S.S.; Chan, H.C.; Lin, Y.C. The effects of sporadic torrential rainfall events on suspended sediments. *Arch. Sci. J.* **2013**, *66*, 211–224.
49. Teng, W.-H.; Hsu, M.-H.; Wu, C.-H.; Chen, A.S. Impact of flood disasters on Taiwan in the last quarter century. *Nat. Hazards* **2006**, *37*, 191–207. [CrossRef]
50. Milliman, J.D.; Syvitski, J.P. Geomorphic/tectonic control of sediment discharge to the ocean: The importance of small mountainous rivers. *J. Geol.* **1992**, *100*, 525–544. [CrossRef]
51. Horowitz, A.J. An evaluation of sediment rating curves for estimating suspended sediment concentrations for subsequent flux calculations. *Hydrol. Process.* **2003**, *17*, 3387–3409. [CrossRef]
52. Thomas, R.B. Estimating total suspended sediment yield with probability sampling. *Water Resour. Res.* **1985**, *21*, 1381–1388. [CrossRef]
53. Wang, Y.M.; Traore, S. Time-lagged recurrent network for forecasting episodic event suspended sediment load in typhoon prone area. *Int. J. Phys. Sci.* **2009**, *4*, 519–528.
54. Chen, S.M.; Wang, Y.M.; Tsou, I. Using artificial neural network approach for modelling rainfall–runoff due to typhoon. *J. Earth Syst. Sci.* **2013**, *122*, 399–405. [CrossRef]
55. Tfwala, S.S.; Wang, Y.M.; Lin, Y.C. Prediction of missing flow records using multilayer perceptron and coactive neurofuzzy inference system. *Sci. World J.* **2013**, *2013*, 584516. [CrossRef]
56. Melesse, A.M.; Ahmad, S.; McClain, M.E.; Wang, X.; Lim, Y.H. Suspended sediment load prediction of river systems: An artificial neural network approach. *Agric. Water Manag.* **2011**, *98*, 855–866. [CrossRef]
57. Kisi, O. Generalized regression neural networks for evapotranspiration modelling. *Hydrol. Sci. J.* **2006**, *51*, 1092–1105. [CrossRef]
58. Wang, Y.M.; Traore, S.; Kerh, T. Computing and modelling for crop yields in burkina faso based on climatic data information. *WSEAS Trans. Inf. Sci. Appl.* **2008**, *5*, 832–842.
59. Lin, J.Y.; Cheng, C.T.; Chau, K.W. Using support vector machines for long-term discharge prediction. *Hydrol. Sci. J.* **2006**, *51*, 599–612. [CrossRef]
60. Leahy, P.; Kiely, G.; Corcoran, G. Structural optimisation and input selection of an artificial neural network for river level prediction. *J. Hydrol.* **2008**, *355*, 192–201. [CrossRef]
61. Martens, J.; Sutskever, I. Learning Recurrent Neural Networks with Hessian-Free Optimization. In Proceedings of the 28th International Conference on Machine Learning, Bellevue, WA, USA, 28 June–2 July 2011.
62. Feyzolahpour, M.; Rajabi, M.; Roostaei, S. Estimating suspended sediment concentration using neural differential evolution (NDE), multilayer perceptron (MLP) and radial basis function (RBF) models. *Int. J. Phys. Sci.* **2012**, *7*, 5106–5177. [CrossRef]
63. Zhang, X.; Yang, Y. Suspended sediment concentration forecast based on CEEMDAN-GRU model. *Water Supply* **2020**, *20*, 1787–1798. [CrossRef]
64. Froehlich, D.C.; Giri, S. Neural Network Prediction of Reservoir Sedimentation. In Proceedings of the 14th International Symposium on River Sedimentation, Chengdu, China, 16–19 September 2019. [CrossRef]
65. Uca, Toriman, E.; Jaafar, O.; Maru, R.; Arfan, A.; Ahmar, A.S. Daily Suspended Sediment Discharge Prediction Using Multiple Linear Regression and Artificial Neural Network. *J. Phys.* **2018**, *954*, 012030. [CrossRef]
66. Nourani, V. Using Artificial Neural Networks (ANNS) for Sediment Load Forecasting of Talkherood River Mouth. *J. Urb. Env. Eng.* **2009**, *3*, 1–6. Available online: <http://www.jstor.org/stable/26203327> (accessed on 21 September 2022). [CrossRef]
67. Sokchhay, H.; Tadashi, S. Using Artificial Neural Network to Estimate Sediment Load in Ungauged Catchments of the Tonle Sap River Basin, Cambodia. *J. Water Resour. Prot.* **2013**, *5*, 111–123. [CrossRef]
68. Qian, L.; Liu, C.; Yi, J.; Liu, S. Application of hybrid algorithm of bionic heuristic and machine learning in nonlinear sequence. *J. Phys. Conf. Ser.* **2020**, *1682*, 012009. [CrossRef]
69. Fallah, S.N.; Deo, R.C.; Shojafar, M.; Conti, M.; Shamshirband, S. Computational intelligence approaches for energy load forecasting in smart energy management grids: State of the art, future challenges, and research directions. *Energies* **2018**, *11*, 596. [CrossRef]

70. Kabir, S.; Patidar, S.; Xi, X.; Liang, Q.; Neal, J.; Pender, G. A deep convolutional neural network model for rapid prediction of fluvial food inundation. *J. Hydrol.* **2020**, *590*, 125481. [[CrossRef](#)]
71. Haurum, J.B.; Bahnsen, C.H.; Pedersen, M.; Moeslund, T.B. Water Level Estimation in Sewer Pipes Using Deep Convolutional Neural Networks. *Water* **2020**, *12*, 3412. [[CrossRef](#)]
72. Ni, C.; Ma, X. Prediction of Wave Power Generation Using a Convolutional Neural Network with Multiple Inputs. *Energies* **2018**, *11*, 2097. [[CrossRef](#)]
73. Samantaray, S.; Sahoo, A. Prediction of suspended sediment concentration using hybrid SVM-WOA approaches. *Geocarto Int.* **2022**, *19*, 5609–5635. [[CrossRef](#)]
74. Nouar, A.; Yusuf, E.; Pavitra, K.; Ali, N.A.; Mohsen, S.; Ahmed, S.; Ahmed, E. Suspended sediment load prediction using long short-term memory neural network. *Sci. Rep.* **2021**, *11*, 7826. [[CrossRef](#)]
75. Taylor, K.E. Summarizing multiple aspects of model performance in a single diagram. *J. Geophys. Res.* **2001**, *106*, 7183–7192. [[CrossRef](#)]
76. Olden, J.D.; Joy, M.K.; Death, R.G. An accurate comparison of methods for quantifying variable importance in artificial neural networks using simulated data. *Ecol. Mod.* **2004**, *178*, 389–397. [[CrossRef](#)]